

Mutations of RhoGDI α have deleterious effect on Glomerular Podocytes and cause Nephrotic Syndrome

David Auguste

Faculty of Graduate Studies

Department of Physiology

McGill University, Montréal, Québec

Submitted in December 2014

A thesis submitted to McGill University in partial fulfillment of the requirements of the degree of Master of Science

© David Auguste, 2014

Table of Contents

Acknowledgements	iv
Abstract	vi
Résumé	viii
Chapter 1: Introduction	1
1.1- The Kidney and the Glomerular Filtration Barrier	1
1.1.1- The Endothelium	1
1.1.2- The Glomerular Basement Membrane	1
1.1.3- The Podocytes	2
1.2- Nephrotic Syndrome	3
1.2.1- Introduction to Nephrotic Syndrome	3
1.2.2- Congenital Nephrotic Syndrome (CNS); Five common genes to cause CNS	3
1.3- Rho-GTPases	4
1.3.1- Roles of Rho-GTPases.....	4
1.3.2- Regulation of Rho-GTPases	5
1.3.2.1- Guanine nucleotide Exchange Factors.....	5
1.3.2.2- GTPase-Activating Proteins.....	5
1.3.2.3- Rho Guanine Dissociation Inhibitors.....	5
Chapter 2: Hypotheses, Research aim and Objectives	8
2.1- Introduction.....	8
2.1.1- The RhoGDI α mutations and the Literature	8
2.1.2- Hypotheses.....	9

2.1.3- Research aims and objectives	9
---	---

Chapter 3: Mutations of RhoGDIα affect podocytes and cause Nephrotic Syndrome	14
3.1- Materials & Methods	14
3.1.1- Materials	14
3.1.2- Cell Culture of Human fibroblasts & mouse podocytes	14
3.1.3- Rho-GTPase Pull-down and Immunoblotting	15
3.1.4- Immunostaining	16
3.1.5- Transfection	17
3.1.6- Fluorescence Resonance Energy Transfer	18
3.1.7- Cell Motility: Wound Healing Assay and Cell Tracking	19
3.1.8- Kymograph	19
3.1.9- Statistical Analysis.....	20
3.2- Results.....	20
3.2.1- Human Fibroblasts.....	20
3.2.1.1- Consequences of Δ D185 Mutation on Cell Functions	20
3.2.1.1.1- Rho-GTPase Pull-down Assay	20
3.2.1.1.2- Motility: Wound Healing Assay	21
3.2.1.1.3- Spatio-temporal observation of Rho-GTPase activity by FRET	21
3.2.1.2- Consequences of Δ D185 Mutation on Cell Morphology and protein distribution	22
3.2.1.2.1- RhoGDI α Localisation.....	22
3.2.1.2.2- Actin Polymerization (Stress Fibre Score and Mean Gray Value	23
3.2.1.2.3- Cell Size and Protrusions	23
3.2.2- Mouse Podocytes	24
3.2.2.1- Consequences of RhoGDI α Mutations on Cell Functions.....	24
3.2.2.1.1- Rescue Establishment and Pull-down Assay	24

3.2.2.1.2- Motility: Wound Healing, Cell Tracking	25
3.2.2.1.3- Altered coordination in extension and retraction of RhoGDI α - defective Podocytes Kymograph.....	25
3.2.2.1.4- Spatio-temporal observation of Rho-GTPase activity by FRET	27
3.2.2.2- Consequences of RhoGDI α Mutations on Cell Morphology	28
3.2.2.2.1- Actin polymerization (F/G-Actin Ratio).....	28
3.2.2.2.2- Elongation and Cell Size.....	29
3.2.2.2.3- Cell Protrusions.....	29
Chapter 4: Discussions	45
4.1- Human Fibroblasts.....	45
4.2- Mouse Podocytes	45
4.2.1- Podocytes' Motility.....	46
4.2.2- Differential hyperactivation of RhoA& Rac1 by RhoGDI α KD & mutant RhoGDI α s	46
4.3- Parallel with human fibroblasts and mouse podocytes.....	49
4.4- Parallel with Pull-down and FRET signal	49
4.5- Parallel with Pull-down and FRET signal	50
Chapter 5: Summary and Conclusion.....	52
5.1- Overall Summary	52
5.2- The parallel with Nephrotic Syndrome	53
References.....	56

Acknowledgements

Many people have contributed in many ways to the completion of this research project. Its realization could not have been the work of any one alone, which is why I wish to extend my special appreciation to all those who provided their help.

First, I would like to direct my deepest gratitude to my supervisor, Dr Takano, for giving me the opportunity to take part of her rewarding and stimulating work. I am particularly grateful to her for being a tremendous guide and great mentor. Her patience and invaluable constructive criticism enhanced my experience throughout the learning process of my Master.

I am thankful to the whole Physiology academic staff for their crucial role in the coordination of the program. Special thanks to Mrs Christine Pamplin who was always there when I was looking for guidance and support on establishing myself at McGill University. It is near to impossible to find someone that answers as quickly and as effectively as her. I also thank Ms Rosetta Vasile and Ms Maria Dimas who are nicely fulfilling the demanding responsibilities of academic coordinator and adviser.

I would like to thank the members of my advisory committee: Dr Erik Cook, Dr John Hanrahan, Nathalie Lamarche-Vane and Dr Louise Larose. Their valuable recommendations allowed me to grow as a future researcher. Dr Lamarche-Vane has also given me much appreciated access to her laboratory for the use of her Fluorescence Resonance Energy Transfer tools.

I could not let this occasion pass by without thanking the research assistants, technicians and post-docs for training me, advising me and facilitating the preparation and accomplishment of my work: Lamine Aoudjit, Cindy Balwin (my great trainer) Dr Takanouri Kumagai, Dr Richard Robins, Dr Erika Hooker, Dr Judith Antoine-Bertrand. I also thank the whole Nephrology Department for the help and support through my journey as a Master student.

Finally, last but definitely not least, I would like to acknowledge with much appreciation the unconditional support of my parents Ulrick Auguste and Elmire Augustin at almost every possible level. They are my lifetime guides, my motivators and my most valuable advisers. Big thanks to my brother and my sister Sébastien Auguste and Emmanuelle Auguste for cheering me up.

Thank you, all!!

Abstract

Background: Congenital nephrotic syndrome (CNS) is featured by heavy proteinuria that occurs within 3 months of age and is caused by genetic mutations that affect glomerular podocyte function. In two sisters with CNS, we identified a deletion of one of three evolutionary conserved aspartate residues (referred to as $\Delta 185$) in *ARHGDI α* , a gene encoding for RhoGDI α . RhoGDI α regulates the activity and intracellular localization of the Rho-family of small GTPases and stabilizes Rho-GTPases in their inactive form. Additional mutations in *ARHGDI α* have since been reported (G173V and R120X) in patients with childhood-onset nephrotic syndrome. The aim of the study was to investigate how the RhoGDI α mutations impact on podocytes' morphology and function. We hypothesized that the mutations cause a reduction or loss of function of RhoGDI α , leading to various cellular defects.

Methods: Immortalized mouse podocytes and human fibroblasts (from control subjects and a patient) were used. Rho-GTPases activity was quantified by pull-down assay. In mouse podocytes, RhoGDI α was knocked-down (KD) by shRNA. KD cells were transfected with mutants or wild type (verified by western blot). Spatiotemporal Rho-GTPase activities were studied by fluorescence resonance energy transfer. Cell motility was analysed with wound healing assay, live cell tracking and kymographs. Analysis of actin cytoskeleton/morphology was done by immunofluorescence staining with Phalloidin and DNASE I and quantification by the ImageJ.

Results: Patient's fibroblasts (expressing $\Delta 185$) showed Rho-GTPase hyperactivation and a blunted response to a RhoA activator. Mouse podocytes with RhoGDI α KD showed hyperactivation of Rho-GTPases, defective motility and morphological changes including reduced F/G actin ratio, smaller and shorter shape, and increased cellular protrusions. These changes were not rescued by the three mutant RhoGDI α s, while the motility was partially rescued by wild-type RhoGDI α . In RhoGDI α KD podocytes expressing the $\Delta 185$ mutant, the Rac1 and RhoA inhibitor restored morphological characteristics and motility, respectively. RhoGDI α KD podocytes showed a deregulation in the coordination of their protrusions' extension-retraction cycle, preventing an optimal motility and migration.

Conclusions: RhoGDI α is a negative regulator of Rho-GTPases and the loss of function mutations lead to hyperactivation of Rho-GTPases. Hyperactivation of Rac1 and RhoA confers differential deleterious impacts on podocytes.

Résumé

Contexte: Le syndrome néphrotique congénital (SNC) est caractérisé par une importante protéinurie qui se développe dès les trois premiers mois de vie. Elle est causée par des mutations génétiques empêchant les podocytes, cellules épithéliales viscérales glomérulaires, d'assumer leur fonction. Nous avons identifié chez deux enfants, sœurs l'une de l'autre, une délétion d'un des trois groupements aspartiques conservés au cours de l'évolution (ci-après dénommée Δ D185) dans *ARHGDI α* , un gène codant pour la protéine RhoGDI α . RhoGDI α régule l'activité et la localisation intracellulaire des GTPases de la famille Rho, les Rho-GTPases. RhoGDI α stabilise les Rho-GTPases sous leur forme inactive. Deux autres mutations (G173V and R120X) ont été rapportées chez des patients parmi lesquels le syndrome néphrotique congénital est apparu pendant l'enfance. La visée de l'étude était d'évaluer l'impact des mutations de RhoGDI α sur la morphologie et la fonction des podocytes. Notre hypothèse stipule que ces mutations au sein de RhoGDI α causent une diminution ou une perte totale des capacités de celle-ci à remplir ses fonctions, menant ainsi au dysfonctionnement de divers processus cellulaires.

Méthodologie : Nous avons utilisé des podocytes de souris immortalisés et des fibroblastes humains. Ces derniers ont été prélevés d'individus contrôles non-porteurs des mutations et d'un des patients initialement mentionnés exprimant Δ D185. Nous avons quantifié l'activité des Rho-GTPases par technique d'immunoprécipitation. Nous avons effectué un knockdown (KD) de RhoGDI α dans les podocytes de souris à l'aide de la méthode d'ARN interférent (shRNA). Des cellules KD ont été transfectées avec les formes mutantes de RhoGDI α ou le type sauvage de RhoGDI α (vérifié par immunotransfert Western). Les activités spatio-temporelles des Rho-GTPases ont été étudiées par technique de transfert d'énergie de fluorescence par résonance (FRET). L'analyse de la motilité des cellules a été effectuée par procédé d'essai de cicatrisation, dit wound-healing assay, et par imagerie des cellules vivantes. Nous avons analysé le cytosquelette et la morphologie des cellules. L'analyse a pu se faire par procédure d'immuno-isolation (immuno-staining) avec la phalloïdine et DNASE I et par analyse sur ImageJ.

Résultats : Les fibroblastes du patient $\Delta D185$ démontrent une hyper-activation des Rho-GTPases et une réponse affaiblie à un promoteur de l'activation de RhoA. Les podocytes de souris à RhoGDI α KD ont mis en évidence une hyperactivation des Rho-GTPases, une motilité déficiente et des changements morphologiques importants incluant une baisse du ratio d'actine filamentueux/actine globulaire, une aire de leur surface plus importante, un facteur d'élongation plus bas, et un nombre plus élevé de protrusions cytoplasmiques. Ces changements n'ont été restaurés par aucun des trois mutants de RhoGDI α . Néanmoins, la motilité des cellules et les facteurs morphologiques observés ont été restaurés par la protéine exogène de type sauvage. Chez les podocytes KD transfectés avec $\Delta D185$, les inhibiteurs de Rac1 et de RhoA ont d'un côté restauré la morphologie et de l'autre restauré la motilité des cellules respectivement. Les podocytes RhoGDI α KD transfectés avec $\Delta D185$ et particulièrement les podocytes RhoGDI α KD démontrèrent un dérèglement dans leur cycle extraction-rétraction de leurs saillies cytoplasmiques témoignant d'un défaut au niveau de la coordination des mouvements nécessaires pour une motilité optimale (incluant celle de pédicelles).

Conclusion: RhoGDI α est un régulateur négatif des Rho-GTPases et des mutations causant sa perte de fonction mènent à l'hyper-activation des Rho-GTPases. L'hyper-activation de Rac1 et de RhoA confère au podocytes des caractères délétères différentiels.

Chapter 1: Introduction

1.1- The Kidney and the Glomerular Filtration Barrier

Located in the lower back just below the rib cage, the kidneys, measuring about the size of a fist, are organs that play major roles in the organism survival. They regulate the blood pressure; stimulate the production of erythrocytes; assure body fluid and metabolites homeostasis. The kidneys are well known for the excretion of wastes through the formation and elimination of urine. They are filters as they keep the important elements that the body needs into the blood stream and excrete unnecessary materials: metabolic wastes, excess of salt, urea, etc. They filter about 200 litres of plasma daily. The fluid equilibrium and the elimination of the waste are regulated through a complex process of filtration, excretion and re-absorption. Every step occurs in specific locations in the structural units of the kidneys called nephrons. The initial stage that forms the primitive urine is relatively simple and happens in the filtration units of the kidneys, the glomeruli (consisting of the Bowman capsule and glomerular capillaries), located in the nephrons. As most filters, the kidneys have a filtration membrane, the glomerular capillary wall, conceived to contribute to an optimal fluid and metabolite homeostasis by retaining cells and proteins into the plasma. The membrane, well known as the glomerular filtration barrier (GFB), is located, as stated in its appellation, in the glomerulus. That perm-selective barrier consists of a triple layer including (from the blood stream to the milieu where the primitive urine is formed) a fenestrated endothelium, the glomerular basement membrane (GBM) and the podocytes [3].

1.1.1- *The Endothelium*

The glomerular endothelial cells are the inner part of the GFB. They represent a very fine layer governing the mechanisms that keep the blood flowing inside the vessels. The endothelium also regulates the glomerular vasomotor tonus. It plays a certain role in the ultra-filtration process. It contains pores called fenestrae (de 70nm à 100 nm) that selectively let go through a large amount of fluid rich in solutes and restrict the passage of most proteins from the blood to the urine [3-5].

1.1.2- *The Glomerular Basement Membrane*

The GBM is the support on which rests most of the glomerular endothelium. It is thicker than most basement membranes. This is due to the fact that it is also the basal membrane of the outer

layer of the GFB, the podocytes. Laminin, type IV collagen, nidogen and heparan sulfate proteoglycan are the main components constituting the GBM [6].

1.1.3- *The Podocytes*

Podocytes are highly specialized differentiated ramified epithelial cells that compose the visceral epithelium of the glomeruli. At the end of their cytoplasmic protrusions we find interdigitating actin-rich foot processes interconnected by a multi-protein slit diaphragm [3, 7]. The podocytes are also rich in microtubules and intermediate filament (the latter is rich in vimentin) that, with the actin cytoskeleton, regulate the podocytes' morphology, rigidity and motility [7, 8].

Nephrin, podocin and Wilms tumour suppressor 1 (WT1) are podocytes specific proteins. Defects on podocytes are often explained by mutations within the genes encoding for these podocyte-specific proteins, such as *NPHS1*, *NPHS2* and *WT1* encoding for nephrin, podocin and WT1 respectively [1]. Other genes are also associated with podocytes injuries when mutated as the proteins that they are encoding for are highly present in podocytes or implicated in podocytes' activities: among these genes we name *LAMB2* encoding for laminin $\beta 2$ and *PLCE1* encoding for phospholipase C ϵ [1, 9]. Podocyte foot processes effacement (disruption of the well-organized structure of interdigitating foot processes) is a common pathological feature in various proteinuric kidney diseases. This witnesses how critical these particular podocytes features are for the normal function of the filtration barrier [8, 10, 11].

The efficient cell-cell interaction and the maintenance of the morphology and motility of the podocytes require a strict regulation of the actin cytoskeleton [8, 9, 12]. Formins, Rho-GTPases and actin-related proteins 2/3 complex are the main actors in the actin dynamics for normal podocytes' function and shape. Of these three families of regulating proteins, Rho-GTPases play the major role in the actin assembly essential for podocytes foot processes to fulfill their critical filtration role [13, 14].

1.2- Nephrotic syndrome

Nephrotic syndrome (NS) is a common kidney disease that is characterized by defects in the GFB. These defects cause an increase of its permeability, causing significant protein loss into the urine [1, 15, 16]. Proteins are the components that the body uses to build and repair tissues and to produce the molecules needed for the organism to function (hormones, enzymes, etc.). Albumin is a protein that drags the supplement of body fluid into the blood stream so it can be eliminated in the urine by the kidneys. A low level of blood albumin due to its leakage in the urine reduces the blood oncotic pressure, thus reduces its proficiency to draw the exceeding body fluid. This eventually causes oedema. Oedema is one of the most common clinical manifestations of NS [1, 16].

1.2.1- *Different forms of Nephrotic Syndromes*

Certain forms of NS can be treated with glucocorticoids and are called steroid-sensitive. This treatment stabilizes the podocytes' actin cytoskeleton. Calcineurin inhibitors are also another drug used to reverse or reduce podocytes' injuries in NS [17]. Other forms of NS do not respond to these treatments and hence are a more serious issue. They are qualified as steroid-resistant [18]. Patients with these forms of NS eventually progress to end-stage kidney disease (ESKD). Some steroid-resistant NS are caused by gene mutations (see below).

1.2.2- *Congenital Nephrotic Syndrome*

The congenital form of the disease, congenital nephrotic syndrome (CNS), is characterized by genetic mutations affecting the podocytes. This form of NS cannot be treated with glucocorticoids or calcineurin inhibitors. The only known therapies to date are dialysis and kidney transplantation [1]. Approximately 80% of CNS cases are caused by mutations in five genes encoding for proteins highly expressed in podocytes: *NPHS1*, *NPHS2*, *WT1*, *LAMB2* and *PLCE1* [1, 9]

1.3- Rho-GTPases

Rho-GTPases are small proteins that operate as molecular switches to control a wide variety of cellular processes. They do so by pivoting between two different conformational forms: the active guanosine triphosphate (GTP) state and the inactive guanosine diphosphate (GDP) state. The Rho family proteins consist of about 20 mammalian members. The most studied mammalian Rho-GTPases are RhoA, Rac1 and Cdc42. They are known to work in collaboration between them to regulate diverse cell functions but they also regulate their proper activities [1, 19, 20].

1.3.1- *Role of Rho-GTPases*

Ras homolog gene family member A, known also as RhoA, is a Rho-GTPase protein of the Ras superfamily encoded by the gene *RHOA*. Like all members of the Ras superfamily, RhoA plays an important role in the cell cycle and cell division. RhoA polymerizes G-actin into F-actin to regulate the cell morphology, motility and polarity. It is well known for its ability to produce stress fibres and its role in transcriptional control. RhoA plays most of its roles via the actions of Rho-associated, coiled-coil containing protein kinase 1 (ROCK1) and diaphanous homolog 1 (DIAPH1) [19, 21].

Ras-related C3 botulinum toxin substrate 1, or Rac1, is a Rho-GTPase of the Rac subfamily encoded by the gene *RAC1* [19]. It regulates a wide variety of cellular activities but is particularly known for its potency to produce cellular protrusions known as lamellipodiae. Rac1 is implicated in cell motility and epithelial differentiation [22, 23].

Cell division control protein 42 homolog, or Cdc42, is another signalling G protein of the Rho-GTPase proteins. It is encoded by the gene *CDC42* [19]. Cdc42 works jointly with Rac1 in cell migration (migratory polarity) and other cellular processes [23]. It is associated with the formation of filopodiae, the endocytosis process and fate specification during cell division [24, 25].

The activity and spatio-temporal distribution of Rho-GTPases are regulated by three groups of molecules: Guanine Nucleotide Exchange Factor (GEF), the activator; GTPase Activating Protein (GAP), the deactivator; and Rho Guanine nucleotide Dissociation Inhibitor (RhoGDI), the stabilizer [19].

1.3.2- Regulation of Rho-GTPases

1.3.2.1- Guanine Nucleotide Exchange Factor (GEF)

Rho-GTPases are unable to exercise any effects on the cells' actin network when they are in the GDP bound form. In order for the Rho-GTPases to be switched on, they need to go through the action of GEFs. GEFs stimulate the activation of GTPases by dissociating the GDP bound to permit the binding of GTP. GEFs can activate Rho-GTPases to take specific actions on the cells. There are over 80 GEFs known in humans. Some have the ability to trigger the activation of multiple Rho-GTPases whereas others have a specific target and can be tissue-specific [26]. For example p63RhoGEF acts only on RhoA and is mainly expressed in the heart and the brain. GEF-H1 and ECT2 are other RhoA GEFs and stimulate RhoA's action on cytokinesis [27, 28].

TrioN and T-lymphoma invasion and metastasis-inducing protein-1 (Tiam 1) are well known Rac1 GEFs [29-31]. Tuba and Intersectin 2 (ITSN2) are Cdc2-specific GEFs [32, 33].

Inhibiting Rho- GEFs is a way to prevent their activities in vitro during different studies. For example, Rac1 inhibitor NSC23766 interacts with TrioN and Tiam 1 to prevent GDP bound to be catalyzed to give away its spot to GTP [30, 31]

1.3.2.2- GTPase Activating Protein (GAP)

Once the Rho-GTPases achieve their functions, they are deactivated by GAPs. GAPs hydrolyse GTP of the active Rho-GTPases in order for them to adopt a GDP non active conformation. As it is the case for GEFs, there are approximately 80 Rho-GAPs in humans with various specificities for Rho-GTPases. To promote Rho-GTPases' activity, targeting GAPs to inhibit GTP hydrolysis is common effective strategy. This is used for example to decrease albumin excretion and attenuate glomerular damage [34-36][, 50].

Inactivation of Rho-GTPases by GAPs once their role is accomplished isn't the last part of the cycle. Rho-GTPases bind to another group of regulator: RhoGDIs [18, 19].

1.3.2.3- Rho Guanine nucleotide Dissociation Inhibitors (RhoGDIs)

Rho-GTPases are not left alone at any point in their off and on cycle. They are either bound to an effector once activated by GEFs or bound to a different protein after their deactivation by

GAPs. Once in their inactive GDP-bound form, Rho-GTPases are generally stabilized by RhoGDIs [1, 37, 38]. RhoGDIs bind to Rho-GTPases after their deactivation and facilitate their rapid shuttling from a membrane, where the actions were needed, to the cytosol. RhoGDIs assure that the Rho-GTPases are not affected by other factors in the intracellular milieu that could disrupt their potency. RhoGDIs assure that Rho-GTPases are preserved from degradation. RhoGDIs also facilitate their shuttling to the membrane when actions are to be taken there (**Figure 1**) [37].

In mammals, there are three known isoforms of RhoGDIs: RhoGDI α , a 204 amino acid protein, also known as RhoGDI1, is ubiquitously expressed and is found in the cytosol of cells. It binds mainly to RhoA, Rac1, and Cdc42 with a higher affinity than the other RhoGDI isoforms; RhoGDI β (Ly-GDI), or RhoGDI2, also called D4, is also found in the cytosol of cells but exclusively in hematopoietic tissues including the bone marrow, thymus, the spleen and the lymph nodes. It counts 201 amino acids. RhoGDI β binds more particularly to RhoA and Cdc42; RhoGDI γ , or RhoGDI3 is found in the Golgi apparatus of lung tissue cells, in the kidneys, the testis, the pancreas. It has an affinity for RhoA, RhoB, RhoG and Cdc42 [37, 39, 40].

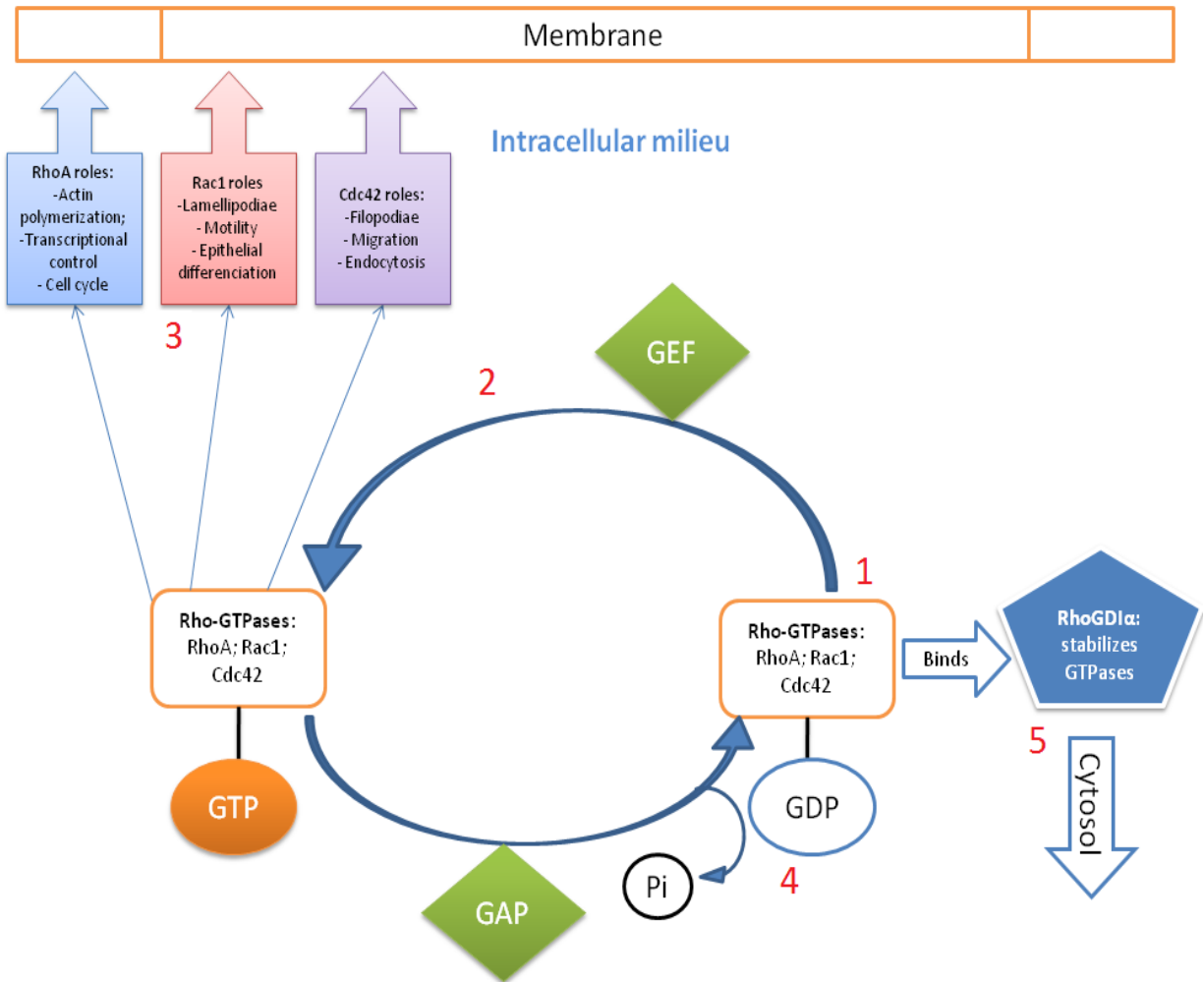


Figure 1: RhoGDI α plays important roles in Rho-GTPases activation-deactivation cycle. Step (1) shows the three mammalian Rho-GTPases RhoA, Rac1 and Cdc42 in their inactive GDP-bound form. When the cell needs some actions to be taken on its cytoskeleton, it gets the cycle going where (2) specific GEFs activate specific Rho-GTPases by eliminating the GDP bond and replacing it with a GTP bond. Rho-GTPases are now switched on and can (3) trigger a wide variety of actions on cell membranes via specific effectors. Once their mission is accomplished, Rho-GTPases are (4) switched off under the action of GAPs where an inorganic phosphate is released and where the GDP state is restored. RhoGDI α (5) stabilises the Rho-GTPases once in their inactive forms and drags them into the cytosol. RhoGDI α can also facilitate the transfer of Rho-GTPases to the membranes.

Chapter 2: Rationale, Hypotheses, Research aim and Objectives

2.1- Introduction

Nephrotic syndrome (NS) is a common kidney disease. It is characterized by defects in the glomerular perm-selective barrier that lead to significant protein loss. The podocyte, a specialized cell type of the glomerular filtration barrier, is known to play an important role in the maintenance of the barrier. Podocyte injury is the main cause of NS [15]. Congenital nephrotic syndrome (CNS) is normally characterized by genetic mutations resulting in defects of the podocytes [1, 41].

2.1.1- The Mutations and the Literature

Performing whole exome sequencing of two siblings with CNS born to consanguineous parents, we identified *ARHGDI A* as a potential gene that, when mutated, could cause the disease. The five genes known to cause CNS, namely *NPHS1*, *NPHS2*, *WT1*, *LAMB2* and *PLCE* were not affected [9, 41]. *ARHGDI A* encodes for RhoGDI α that is known to regulate Rho-family of small GTPases thereby regulating various cellular processes that deal with the organization of the actin cytoskeleton. This protein helps to dictate cell fate and other cellular activities. It is indubitable that its roles are highly significant. The mutation is a deletion of one of three evolutionary conserved aspartates (positions 183/184/185). Since we don't know which of the three aspartates has been deleted, we will refer to that mutation using the term $\Delta D185$. The D residues at position 184 and 185 are localized at the interface where RhoGDI α binds to Rho-GTPases [1], thus it is likely that the deletion mutation would affect its interaction with Rho-GTPases. In addition to CNS, the patients had other critical pathological conditions. RhoGDI α is ubiquitously expressed and the patient has many affects that are not limited to the kidneys. This is building confidence on the fact that the mutation is at least partially responsible for the development of CNS [37]. A previous study showed that the knockdown of RhoGDI α in mice causes many abnormal phenotypes including nephrotic syndrome-like proteinuria. The mice died of renal failure within a year [42]. The results are consistent with the speculation stating that a loss-of-function mutation of RhoGDI α would cause NS.

Other mutations within the same gene have since been reported in patients with NS: A replacement of a G residue by a V residue at position 173, and a truncation of all the residues

following the arginine at position 120. These mutations will be referred to as G173V and R120X respectively [43].

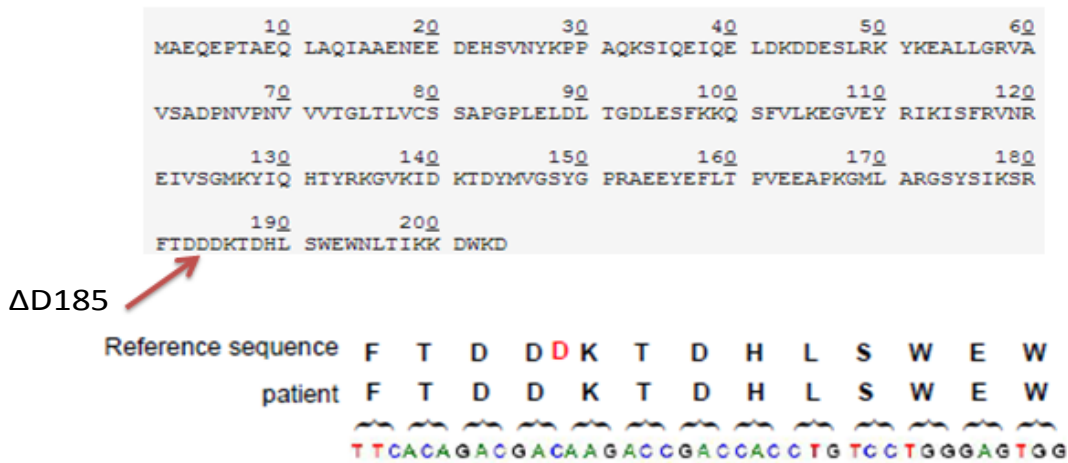
2.1.2- Hypotheses

Following the findings mentioned above, we hypothesized that *ARHGDI*A mutations (Δ D185, G173V and R120X) cause loss or reduction of RhoGDI α 's function which translates into a hyperactivation of Rho-GTPases. We expected an attenuated activation of the Rho-GTPases upon stimulation in mutant-carrying cells. Since Rho-GTPases are powerful regulators of the actin network, we anticipated impairment of the motility and alterations of the actin cytoskeleton along with alterations in the morphology of the mutant-carrying cells.

2.1.3- Research aims and objectives

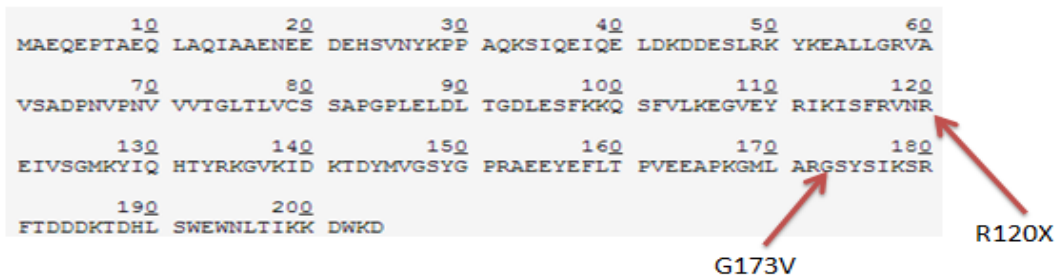
We characterized primary skin fibroblasts derived from one of the affected children and established the functional consequence of this mutation. Fibroblasts from healthy children of the same age group were used as control to reduce the disparities caused by extraneous variables (Selection). We studied Rho-GTPases' activity by pull-down assay. We expected that the Rho-GTPases would co-immunoprecipitate with the RhoGDI α of the control cells but not that of the patients' cells. RhoGDI α localization has been studied by immunostaining. A mislocalization of the mutant form of RhoGDI alpha was expected with respect to the control cells. We also assessed a spatio-temporal profile of Rho-GTPases' activity by fluorescence resonance energy transfer (FRET). We believed that the ability of mutant RhoGDI α to stabilize RhoGTPases into an inactive form would either not occur or would be reduced: the fraction of active RhoGTPases should be higher thus their total amount (active and inactive forms) should be less. We predicted that, following stimulation of one of these RhoGTPases, the increase in activity shouldn't be as important for the mutant-carrying cells as it will be for the control cells. Cell motility by wound healing assay and live cell tracking has been analyzed. Because RhoGTPases are key regulators of cell motility, we expected that mutant-carrying cells would exhibit defective motility compared to that of control cells. For the second part of the research project, we used the same analytical tools to characterize cultured mouse podocytes in which RhoGDI α is knocked-down by shRNA. Rescue experiments were performed in these cells with both wild-type and the three mutant forms of RhoGDI α . We established the morphological consequences of *ARHGDI*A

mutations on podocytes by studying the actin cytoskeleton of cells stained with phalloidin-Alex-fluor 555 and DNASE I 594 (plus DAPI) and by generating kymographs for a more in depth examination of changes in the cytoskeleton.



Gupta et al. J Med Genet, 2013

*ARHGDI*A mutations cause nephrotic syndrome via defective RHO GTPase signaling



Gee et al. J Clin Invest, 2013

Figure 2: Location of RhoGDI α mutations. The top panel shows where the Δ D185 mutation occurred (on an intact full sequence of RhoGDI α). The reference sequence emphasises the positioning of the evolutionary conserved D residues. The arrows in the bottom panel show where the G173V and R120X mutation occurred.

ΔD185	<ul style="list-style-type: none"> • One of three evolutionary conserved D residue normally found at position 183, 184 or 185 is missing
G173V	<ul style="list-style-type: none"> • A G residue at position 173 has been replaced by a V residue
R120X	<ul style="list-style-type: none"> • The RhoGDIα protein is missing the rest of its amino acids chain after the R residue at position 120

RhoGDI Mutants clinical phenotype		
<p>ΔD185:</p> <ul style="list-style-type: none"> - Early life severe CNS - Small glomeruli, - Hypercellularity - Mesangial sclerosis - Simplification and the solidification of glomerular tuft - Immature, hypertrophic, vacuolated podocytes - Tubulo-interstitial changes. - Progression to ESKD* 	<p>G173V:</p> <ul style="list-style-type: none"> - Early- onset NS - Diffuse mesangial sclerosis (DMS) - Foot process effacement 	<p>R120X:</p> <ul style="list-style-type: none"> - Early- onset NS - Diffuse mesangial sclerosis (DMS) - Foot process effacement

Table 1: General characteristics of RhoGDI α mutations and clinical phenotypes. The top part of the table recapitulates the changes in RhoGDI α according to the mutations examined. The bottom part of the table enumerates characteristic phenotypes of patients with the mutations.

*ESKD stands for End-stage kidney disease

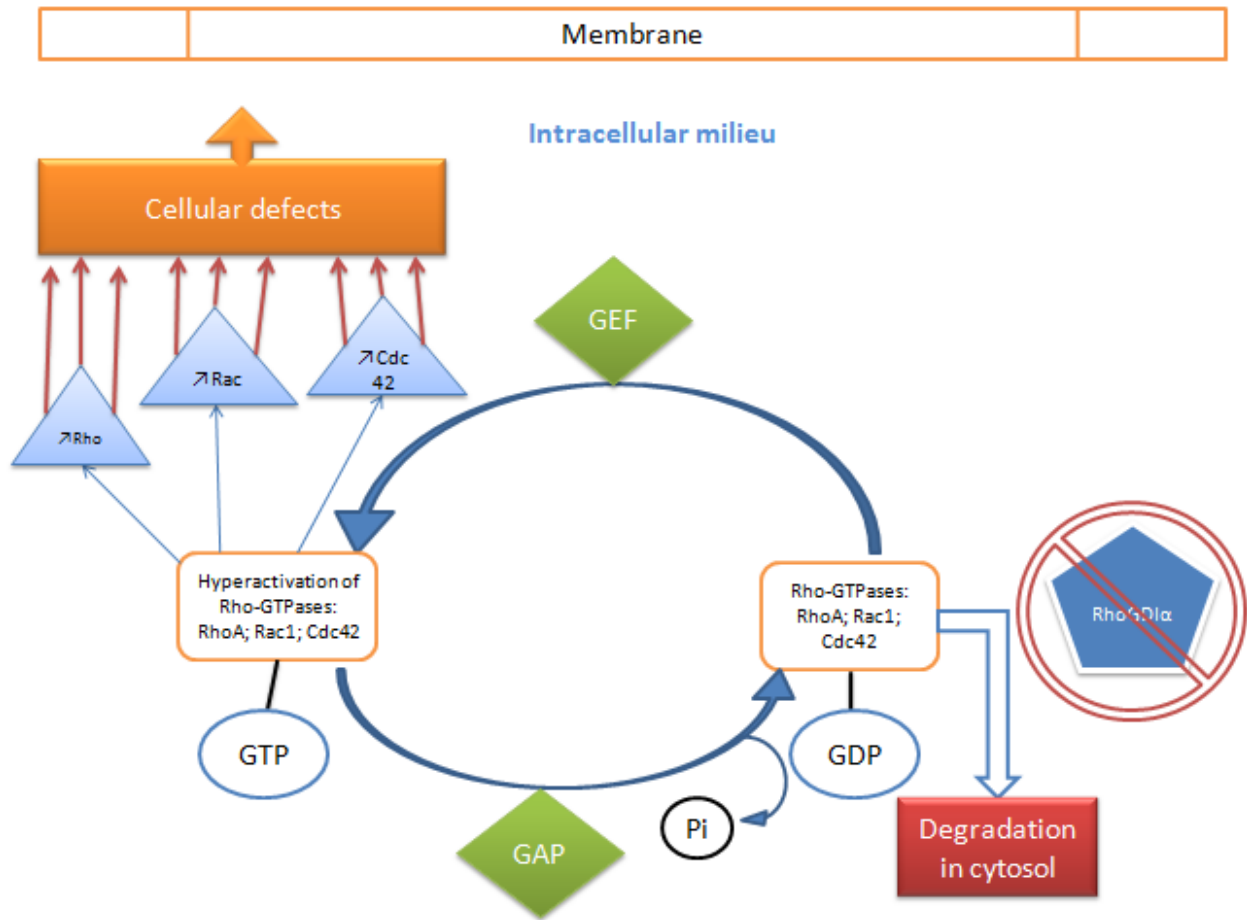


Figure 3: Mutations of RhoGDI α may mimic the consequences of RhoGDI α knockdown. RhoGDI α generally stabilizes the inactive GDP-bound form of Rho-GTPases and facilitates their rapid shuttling to and from the membranes. The absence of RhoGDI α leads to hyperactivation of Rho-GTPases causing cellular defects. Mutations of RhoGDI α affect its ability to regulate Rho-GTPases which may provoke defects similar to those seen in RhoGDI α KD cells.

Chapter 3: Mutations of RhoGDI α affect podocytes and cause Nephrotic Syndrome

3.1- Materials & methods

3.1.1- Materials

Antibodies for RhoGDI α (A-20 rabbit polyclonal IgG), green fluorescence protein (GFP) (B-2 mouse monoclonal IgG_{2a}) and tubulin (mouse) were purchased from Santa Cruz Biotechnology (Dallas, Texas). The Fluorescein Isothiocyanate (FITC) secondary antibody (goat anti-rabbit) was from Cedarlane Laboratories (Burlington, Ontario). Anti-rabbit IgG Fab2 Alexa Fluor 488 was from Cell Signaling Technology (Danvers, Massachusetts). The Glutathione Sepharose was from GE Healthcare Bio-Sciences (Baie d'Urfé, Québec). DNASE I-Alexa Fluor 594 was from Molecular Probes (Eugene, Oregon). G418, puromycin, Alpha MEM, DMEM, Phosphate Buffered Saline (PBS), Foetal Bovine Serum (FBS) and RPMI were purchased from WISENT Inc. (Saint-Bruno, Québec). Interferon γ (IFN- γ) was from Life Technologies (Burlington, Ontario). Electrophoresis reagents for Western Blots were from BioRad (Mississauga, Ontario). Collagen type I was from Sigma (Santa Fe, New Mexico). Opti-MEM and penicillin-streptomycin were purchased from Life Technologies (Burlington, Ontario). PFA was from Thermo-Scientific (Waltham, Massachusetts). Horseradish peroxidase was from Immuno Jackson (West Grove, Pennsylvania). Rac1 inhibitor, NSC23766, was from Tocris Bioscience (Ellisville, Missouri). The RhoA inhibitor, C3 transferase, was from Cytoskeleton (Denver, Colorado). The 40,6-diamidino-2-phenylindole (DAPI) was purchased from Invitrogen (Burlington, Ontario).

3.1.2- Cell culture of Human fibroblasts and mouse podocytes

The human fibroblasts obtained from the CNS patient with the Δ D185 mutation and from control individuals (MCH058 and MCH065) were described previously and were maintained in Alpha MEM containing 10% FBS [1]. Mouse podocytes were maintained in RPMI at 33 °C with Interferon γ and were transferred at 37 °C for differentiation. The original SMP (Shankland Mouse Podocyte) mouse podocytes were obtained from Dr. Shankland (University of Seattle) [44]. The cell lines were established as described in transfection section. Puromycin was used to keep the selection of cells with the viral vector of lentivirus containing shRNA of interest (in our case used to silence RhoGDI α expression. We used the empty vector for control cells). All

rescued cells were cultured with G418 to keep the selection of pEGFP-N1. Another mouse podocyte line (KPN) from Dr Kopp (NIDDK) was maintained in DMEM [45].

3.1.3- Rho-GTPase Pull-down and Immunoblotting

The active form of Rho-GTPases was pulled down using the Rho-binding domain of rho-kinase (RBD) fused to GST (glutathione S-transferase) beads (GST-RBD) for RhoA and the Cdc42-Rac1 Interactive Binding domain fused to GST beads (GST-CRIB) for Rac1 and Cdc42, as described previously [46].

Preparation of GST Proteins: Competent E. coli BL21 was transformed with GST-RBD and GST-CRIB and plated on agarose plates. Colonies were inoculated and left overnight to grow in 50ml of LB with 100µg/ml Ampicillin (LB/Ampicillin) at 37 °C. The culture is then diluted at 1/20: 50ml in 1 l of LB/Ampicillin. The culture was left at 37 °C for 2 hours. The bacteria were induced with 0.1nM IPTG for 3 hours at 30 °C for GST-RBD and at 37 °C for GST-CRIB. The cultures were collected and centrifuged at 4000 RPM for 15 minutes at 4 °C.

On ice, the bacterial pellets were rinsed with 10ml of STE (Sodium Chloride Tris-EDTA) buffer. We then centrifuged the pellets for 10 to 15 minutes at 3000 RPM at 4 °C before lysis and sonication process in 20 mM HEPES (pH 7.5), 1% NP-40, 120mM NaCl, 2 mM EDTA, 10% glycerol, 10 µg/ml aprotinin, 10 µg/ml leupeptin, 1 mM PMSF. Sonication was done 3 times for 30 seconds with 1 minute of stoppage between each. Following sonication, pellets were centrifuged for 20 minutes at 10000 RPM in a 14ml tube with snapping cap. The lysate was collected and resuspended in 0.5% NP40 final.

Purification of GST beads bound to proteins: The supernatant was collected with 300µl of GST beads and put on rotator for 30 minutes at 4 °C. The beads were rinsed two times with lysis buffer and kept at 4 °C (not more than 15 days). To dose the amount of proteins, 10µl of 10% gel was added with BSA. (BSA was used as standard for SDS-PAGE).

Pull-down: The cells were rinsed with PBS and lysed in 500µl of lysis buffer on ice. The lysates were collected in cold sterile 1.5ml eppendorf tubes and centrifuged 30 seconds at 14,000 RPM. The supernatants were collected in another sterile eppendorf tubes. Extraction was done with 20µl of GST beads.

The aliquots of the precipitates were subjected to SDS-PAGE then to immunoblotting using Rho-GTPase antibodies, RhoA, Rac1, or Cdc42. Total cell lysates were also immunoblotted for RhoGDI α and tubulin. Signals were visualized with enhanced chemiluminescent (ECL) using horseradish peroxidase as substrate.

3.1.4- Immunostaining

RhoGDI α staining: Human fibroblasts from MCH058, MCH065 and CNS individuals were cultured in collagen Type I treated cover glasses and were serum starved overnight prior to staining. Cells were washed in PBS then fixed in 4% PFA (Paraformaldehyde) in PBS for 15 minutes. The cover glasses were then left in PBS three times for 3 minutes each before being treated with 0.1% Triton (in PBS) for 3 minutes. After three 3 minute-rinses with PBS, the cover glasses were treated with anti-RhoGDI α Rabbit Ab (2 μ g/ml) for 45 minutes. After the first antibody treatment, glass covers were rinsed three times for 3 minutes before the application of the second antibody (Anti Rabbit) for 1 hour. The following step, after another three-time rinse round, was to stain the cells' F-actin cytoskeleton using Alexa Fluor Phalloidin 555 (at 40 μ M) for 20 to 25 minutes in PBS. The covers were washed again three times for three minutes each time then the nucleus was stained using DAPI for 1 minute (at 0.1 μ g/ml). After one three-minute rinse, the cells were mounted and placed at 4 $^{\circ}$ C overnight. The next day the slides were ready for microscopy.

F-actin to G-actin ratio staining: Mouse podocytes (SMP) were prepared for staining as previously described for human fibroblasts. They were serum starved overnight, washed in PBS, fixed in 4% PFA in PBS then rinsed again before being permeabilized with Triton 0.1%. Cells were treated with Alexa Fluor-555 phalloidin to stain F-actin and Alexa Fluor 594 DNASE I (at 0.3 μ M) for G-actin for 25 minutes. After washing them, cells were stained with DAPI and washed once more. The mounted slides were left to dry overnight at 4 $^{\circ}$ C. Pictures of the cells were taken using LSM780 Zeiss confocal microscope using two lasers (564 and 631 to avoid overlaps between Phalloidin and DNase I fluorescence). Once acquired, the pictures were analysed using ImageJ. The intensity of the phalloidin staining and the DNase I for a certain amount of cells per cell line was measured by selecting cells one by one and tracing their contour. Once we acquired the intensity of phalloidin (F- actin) and DNase I (G-actin), we divided F-actin values by G-actin values respectively to each cells. This gives the F-actin to G-actin ratio.

3.1.5- Transfection

The knock down by shRNA: The shRNAs directed to human RhoGDI α and control shRNA were packaged using the packaging vector psPAX2 and the envelop vector pMD2.G in transducer HEK 293T cells.

We plated 7×10^5 293T cells in 5 ml of DMEM with 10% FBS in a 60mm culture dish. Cells were incubated at 37°C 5% CO₂ overnight. The next day, two tubes (identified as 1 and 2) were prepared for transfection. In tube 1 we added 3 μ l of Lipofectamine 2000 and 77 μ l OPTI-MEM and we left it incubating for 5 minutes. Meanwhile, in tube 2 we added 1 μ g of our shRNA of interest, 750 ng of psPAX2 packing plasmid, 250 ng pMD2.G plasmid envelop and 20 μ l OPTI-MEM. The content of Tube 1 and 2 were mixed after 5 minutes of incubation time of Tube 1. The mixed contents of tube 1 and tube 2 were left incubating for 20 to 30 minutes. The mix was then added to the culture dish of 50%-80% confluent 293T cells (100 μ l per plate). Incubation time following the addition of the mix should be at least 12 hours and should not exceed 15 hours.

After 12-15 hours of incubation, the cells were washed with PBS before a change of medium (DMEM with 10% FBS and penicillin 1%). Cells were left incubating overnight. The next day we harvested the media (which now contains the lentiviral particles) from the cells and transferred it to a polypropylene storage tube. The media must be stored at 4°C.

Fresh media (DMEM with 10% FBS and penicillin 1%) was added to the cells and the cells were then placed in the incubator at 37°C, 5% CO₂ for 24 hours. After the incubation time we harvested the media from the cells and with pooled it with the previously harvested media. The lentiviral media was filtered through a 0.45- μ m-minipore filter to remove all the cells.

The mouse podocytes must be approximately 70% confluent for transduction with virus. Prior to transduction, the mouse podocytes are rinsed and maintained in fresh RPMI with 10% FBS. To each 60mm plates, 1ml of lentiviral media was added (with RhoGDI α shRNA or control shRNA) with polybrene at 8 μ g/ml. The cells were incubated overnight at 37°C, 5% CO₂. After 24 hours of infection, the medium was changed to a fresh one. After 72h, puromycin (0.3 μ g/ml) was added for the selection of the cells successfully transfected. After selection, we expanded the mouse podocytes for our studies.

Other Transfection with Lipofectamin 2000: Two solutions, A and B, were prepared. One with the diluted plasmid, the other with diluted Lipofectamine 2000. In a sterile 1.5ml tube, the plasmids needed for each experimental condition was added. For a 35mm dish, 0.1 μg to 0.3 μg of plasmid was used. The plasmids were diluted in 100 μl Opti-MEM (100 μl per dish); Solution B contained 100 μl of Opti-MEM for each 35mm dish. About 3 μl of Lipofectamine 2000 was added per μg of DNA to be transfected.

Solutions A and B were mixed within no more than 5 minutes of solution B preparation. The mixed solution was then left at room temperature for 20 minutes. During the 20 minutes the cells to be transfected were rinsed with PBS then left in 1ml Opti-MEM (for 35mm dish). After the 20 minutes, a fraction of the mixed solution was added to each dish (at equal volume for equal amount of DNA to be transfected) that is 200 μl for one 35mm dish. Cells were left 4 hours in solution then rinsed and incubated with Alpha MEM with 10% FBS for human fibroblasts or RPMI with 10% FBS for SMP mouse podocytes.

For the FRET transfection experiment, human podocytes were left in Alpha MEM with 10% FBS the second and third days and serum starved in Alpha MEM with 0.5% FBS overnight of the third day. The fourth day, the day of acquisition, human fibroblasts were placed in FBS free Alpha MEM. The same has been done with SMP cells but with RPMI instead of Alpha MEM.

3.1.6- Fluorescence Resonance Energy Transfer

Human fibroblasts- control cells (MCH058 & MCH065) and CNS (Mutant)- were transfected with probes respective to the GTPase of interest: Raichu-1502 for RhoA and Raichu-CRIB (1015) for Rac1 and Cdc42 (no FRET probe to differentiate Rac1 and Cdc42 activation are currently unavailable). We induced the activation of the GTPases with Calpeptin (2 μM) or Epidermal Growth Factor (100nM) (EGF) for RhoA and Rac1/Cdc42 respectively. Following overnight serum-starvation, fluorescence images of the cells were acquired every 2 minutes for 10 minutes by an inverted fluorescent microscope (IX81; Olympus): an acquisition was done at time 0 (zero) and after activation with the respective stimulator (calpeptin for RhoA and epidermal growth factor for Rac1/Cdc42). To present the results in a quantitative manner, the intensity of the fluorescence of the cells at each time point was measured using Metamorph BioSoftware. The software was set to obtain normalized FRET values for each pixel following

the principal where raw FRET values minus background were divided by respective CFP values minus background. The intensity was converted to pseudocolor to visualize spatial profile of Rho-GTPase activities [47]. The average FRET intensity of each cell over the time was then plotted against the time (from time 0 to 10 minutes) and a linear trend line was used to calculate the slope of the change in FRET values. We used the average slope for each line and we entered the values in a graph with error bars. In our case, the slope describes the overall direction of the activation/deactivation (increase-decrease, positive-negative- neutral) of the Rho-GTPases following stimulation and the intensity of the FRET signal (the further from Zero the number is the more varying is the FRET activity). In other words, here a negative slope value, relatively far from 0 represents a high Rho-GTPase activity.

3.1.7- Wound Healing Assay and Cell Tracking

Cells were serum starved overnight prior to performing the experiment in Alpha MEM containing 0.5% FBS. Two straight scratches were made on a 100% confluent layer of cells using a 10 μ l pipette tip. The cell layer was washed with PBS to remove the detached cells. Lines were marked at the bottom of the dishes and used as reference areas where photos were taken at time 0 and time 24h. The wound surface area was measured at both time points. The percentage of the wound closure was then calculated. The average of four wound areas per dish was used to calculate the average wound healing for four to six sets of experiment.

For the live cell tracking experiment, following overnight serum starvation, cells were imaged every 10 minutes for three hours with a brightfield Axiovert microscope. Their positions through the time were tracked and the total distance and displacement were traced and measured using Zen (ZEISS Efficient Navigation) Imaging Software. The average cell displacement and average distance they covered were calculated for each cell line.

3.1.8- Kymographs

Mouse podocytes were transfected with mCherry-tagged actin using lipofectamin 2000. Live cell images were acquired using a confocal microscope (LSM780 Zeiss) every 15 seconds for 20 min. The MultipleKymograph plugin for ImageJ was used to generate kymographs. The plugin and the instructions needed to create and analyze the kymographs can be found on http://www.embl.de/eamnet/html/body_kymograph.html.

3.1.9- Statistical Analysis

The data are presented as the mean values acquired from multiple set of experiment with standard errors. For comparison of variables between two groups, the statistical significance was assessed by a *t* test using IBM SPSS Software (Armonk, New York) or Microsoft Excel. For the comparison of variables between more than two groups, statistical significance was assessed by One-way Anova. Post Hoc analysis was launched when significance was reached at $p < 0.05$: we used the Tukey's range test using the IBM SPSS Software.

3.2 Results

3.2.1- *Human Fibroblasts*

It was less difficult to get skin fibroblasts than podocytes from a biopsy of living human on a technical point of view but also ethically. Since RhoGDI α is expressed in all cells, the mutant $\Delta 185$ was available for study. The skin fibroblasts are also relatively easy to keep in culture.

3.2.1.1- Consequences of $\Delta 185$ mutation on Cell Functions

3.2.1.1.1- Hyperactivation of Rho-GTPases in $\Delta 185$ Human Fibroblasts

Since RhoGDI α is an important regulator of Rho-GTPases activation/deactivation cycle, we were interested in the basal level of activity of RhoA, Rac1 and Cdc42. We hypothesized that the Rho-GTPases' activity will be increased in CNS cells compared to control cells. We performed a pull-down assay of the active RhoA (aRhoA), the active Rac1 (aRac1) and the active Cdc42 (aCdc42). We assayed aRhoA with rhotekin Rho binding domain (RBD) and aRac1 and Cdc42 with Pak1 Cdc42 and Rac interactive binding domain (CRIB). On the right panel in **Figure 4A** are shown the total lysates. Note that RhoGDI α protein was expressed at the same level in all three MCH058, MCH65 and CNS fibroblasts lines. Despite seeing more total RhoA, Rac1 and Cdc42 in both control fibroblast lines compared to CNS fibroblasts, we observed a higher basal level of activated Rho proteins in CNS fibroblasts. The experiment was previously done on mouse podocytes using a control line and a RhoGDI α knockdown line [1]. The changes that the

mutant Δ D185 RhoGDI α brought in the level of activity of Rho-GTPases in fibroblasts were comparable to what was induced by RhoGDI α knockdown in mouse podocytes. This suggests that the Δ D185 mutation provokes a loss or reduction of function of RhoGDI α .

3.2.1.1.2- Affected Migration of Δ D185 fibroblasts

A disrupted motility is associated with a deregulation of Rho-GTPases activity. We wanted to analyse the impact that the Δ D185 RhoGDI α mutation would have on cell motility. We did a wound healing assay of all three MCH065, MCH058 and CNS fibroblast lines. We measured the wounds' surface area at time 0 and 24 hours later at the same spots. We calculated the percentages of healing through 24h hours and observed that both control lines, MCH065 and MCH058, migrate significantly faster than the patients' fibroblasts (**Figure 4B**).

3.2.1.1.3- Spatio-temporal observation by FRET

In the interest of assessing a spatio-temporal profile of Rho-GTPase activities to study subcellular distribution of the Rho-GTPase activities, we used the non radioactive live cell imaging technique, fluorescence resonance energy transfer (FRET). Based on the pull-down assay results, we expected that the ability that the mutant RhoGDI α has to stabilize RhoGTPases into an inactive form will be reduced. The fraction of active RhoGTPases should be higher while the total amount of Rho-GTPases (inactive + active) would be reduced as a consequence of the reduced protein stabilizing effect of RhoGDI α . Predictions were that, upon stimulation of these Rho-GTPases, their increase in activity may not be as prominent in the cells carrying the Δ D185 RhoGDI α mutant as it would be for the control cells since available RhoA, Rac1 and Cdc42 (inactive) are found at a lower level in mutant cells. Inactive RhoA (from total lysate) is lower due to its hyperactivation. We transfected a set of control fibroblasts and CNS fibroblasts with the RhoA probe Raichu-1502 and another set of the three cell lines with Raichu-1015 for Rac/Cdc42. Note that the probe of interest binds to the active form of the targeted Rho-GTPase and reduces the FRET signals. The emitter (CFP) and the receiver (YFP) are initially in contact. When active, Rho proteins bind to CFP and YFP, which causes them to separate from each other, hence decreasing the FRET signal (**Figure 5A**). Therefore, a low FRET signal will correspond to a high RhoA activity. **Figure 5B** is the FRET bar showing the FRET signal intensity and the corresponding Rho-GTPases activity. We stimulated RhoA using Calpeptin. Calpeptin inhibits

calpain, a protein that degrades RhoA. Epidermal Growth Factor (EGF) stimulates cell growth and other cellular processes via the action of Rac1 and Cdc42, thus we used EGF to stimulate the activation of these two Rho-GTPases. **Figure 5C** is an example of the acquisition of the FRET signal at time 0 and every 2 minutes for 10 minutes following stimulation. We quantified the evolution of the FRET signal using the slopes obtained from graphs in which we entered the values of the intensity per time lapse. The slope gives information on the change in the intensity of the FRET signal (steepness) and on the direction of the evolution of the signal (positive, negative or neutral if equal to 0). RhoA activity increased (FRET signal decreased) significantly more upon calpeptin stimulation in both control fibroblasts compared to CNS fibroblasts (**Figure 5D**). This implies that there is initially less GDP-RhoA due to the absence of RhoGDI α action to keep them in its inactive state in CNS fibroblasts. There is less RhoA to be activated.

Even though the trend was the same for Rac1 and Cdc42 (where the increase in activity is weaker in CNS fibroblasts than in both control fibroblasts), the difference was not significant (**Figure 5E**).

The Pull-down revealed higher Rho-GTPase activities in CNS cells (**Figure 4**). The FRET signaling showed a weaker RhoA activation upon stimulation in these fibroblasts (**Figure 5**). We then expected to see a lower baseline FRET signal (a higher RhoA, Rac1 and Cdc42 activity) in CNS fibroblasts. We calculated the average time 0 FRET signal (baseline) for all three cell lines. Interestingly we haven't seen any significant difference (Figure not shown).

3.2.1.2- Consequences of Δ D185 mutations on Cell morphology and protein distribution

2.3.1.2.1- Mislocalization of RhoGDI α in Δ D185 Fibroblasts

By immunostaining, we wanted to determine if the intracellular localization of the mutant form of RhoGDI α differs from that of the wild type form. RhoGDI α is normally localized in the cytosol of all cell types. We stained human fibroblasts with Alexa Phalloidin (Red) and DAPI (Blue) to delimit the cells and select those that are not dividing, or growing on top of another. The cells were also stained for RhoGDI α (Green). In CNS fibroblasts, RhoGDI α was often found in the nucleus. We counted cells in five random areas on the slides for all three CNS, MCH065 and MCH058 lines and we quantified the percentage of cells in which RhoGDI α was found in

the nucleus. In 85% of the CNS fibroblasts, RhoGDI α was localized in the nucleus, compared to 7% to 13% for MCH065 and MCH058 (**Figure 6A**). Thus, the mutation of RhoGDI α has affected its ability to maintain its normal cytosolic localization in the cells. This could be due to a reduction of charges and or reduction in the affinity to its regular partners or an increased capacity to reach uncommon cellular areas.

3.2.1.2.2- Affected actin polymerization in Δ D185 Fibroblasts

RhoA is known to facilitate the formation of stress fibres. An increase in the activity of RhoA would be consistent with an increase in stress fibres. In order to verify this, we used a Stress Fibre Score (SSS). The SSS is on a 0 to 3 scale where 0 indicates the absence of stress fibre; a score of 1 is given when the stress fibres occupy a lot less than 50% of the cell surface; the score is 2 when the stress fibres cover about 50% of the cell; a SSS of 3 is attributed to cells when the stress fibres cover much more than 50% of the cell surface. **Figure 6B** shows representative pictures of the stress fibre level in control fibroblasts and CNS Fibroblasts. We evaluated the SSS of 60 to 72 cells per cell lines. The SSS analysis indicates a significant higher amount of stress fibres in CNS fibroblasts compared to both control lines as predicted (**Figure 6C**).

To analyse the action of RhoA on the actin polymerization in a more objective manner, we adopted the Mean Gray Value (MGV) measurement. We measured the intensity of the Phalloidin staining of human fibroblasts using ImageJ. We expected a higher MGV in CNS fibroblasts than in control cells. We obtained the same trend as in the SSS where the values for CNS were much higher (**Figure 6D**). The difference between CNS and MCH058, however, was not quite significant ($p = 0.098$).

3.2.1.2.3- Affected Δ D185 fibroblasts size and protrusions formation

The surface area of CNS fibroblasts tends to cover more grounds (though not significant) than both control fibroblast lines, MCH065 and MCH058 (not shown). More again, Rac1 is known to stimulate the formation of lamellipodiae and Its hyperactivation could translate into an increase number of lamellipodiae. In order to verify that, we counted the protrusions in over 50 cells for each MCH058, MCH065 and CNS Fibroblasts lines and calculated the average protrusions per cell. There was no significant difference in the number of lamellipodiae among the three fibroblast lines (**Figure 7A**).

3.2.2- Mouse Podocytes

Podocytes are the cells that are particularly affected in NS. Studying the mutations in podocytes is thus more directly relevant to understanding the pathogenesis of NS induced by RhoGDI α mutations. We conducted a series of experiments on mouse podocytes to get a better insight of the pathogenesis.

3.2.2.1- Consequences of RhoGDI α Mutations on Cell Functions

3.2.2.1.1- Rescue Establishment and Pull-down Assay

We prepared 6 different mouse podocyte lines using cells obtained from Dr. Shankland as a parental line [44]. We developed a control line expressing the empty viral vector; GDI KD line that is stably expressing an shRNA against mouse RhoGDI α (GDI KD); GDI KD stably transfected with Δ D185 mutant RhoGDI α (human, GFP-tagged); GDI KD stably transfected with G173V RhoGDI α (human, GFP-tagged); GDI KD stably transfected with R120X RhoGDI α (human, GFP-tagged); and RhoGDI KD stably transfected with WT RhoGDI α (human, GFP-tagged) [1]. The western blot in **Figure 8A** shows successful KD and RhoGDI α mutants rescue. RhoGDI α and GFP each have a molecular size of ~25kDa. Thus GFP-tagged RhoGDI α s have a 50kDa size except the GFP-tagged RhoGDI α R120X mutant. Because of the truncation, RhoGDI α of this mutant is about half the normal size which is why when tagged to GFP it is ~37kDa. The weak bands seen at ~25kDa in the mutant cell lines lane are likely resulting from the degradation of the GFP-Tagged RhoGDI α . **Figure 8B** shows the rescue with the WT form of RhoGDI α .

In mouse podocytes, the total lysate levels of RhoA, Rac1 and Cdc42 are higher in control cells than in RhoGDI α KD and all three mutant cells. When it comes to GTP-bound Rho-GTPases, we note that they tend to be at a higher level in RhoGDI α KD and mutant-carrying podocytes than in control podocytes (**Figure 9A**). **Figure 9B** is a quantification of the level of active RhoA, active Rac1 and active Cdc42. Rac1 is most consistently hyperactivated in RhoGDI α -defective cells. RhoA activity is significantly higher in RhoGDI α KD and Δ D185 podocytes, as compared with control. The difference is not significant when we compare the RhoA levels of G173V and R120X mutants to that of control. The difference between Δ D185 and G173V could be explained

by the fact that the mutation in G173V is not at the interface where RhoGDI α interacts with Rho-GTPases contrarily to Δ D185. The impact of the mutation might not be as deleterious on RhoGDI α functions' in G173V podocytes as in Δ D185 podocytes. Contrarily to RhoA and Rac1, Cdc42 levels were inconsistent from a cell line to another. This is why experiments were carried on analyzing from a RhoA and Rac1 point of view.

3.2.2.1.2- Affected Migration of mutant RhoGDI α - carrying Podocytes

Knowing that Rho-GTPases are key regulators of cell motility, we wanted to determine if the pattern of the motility of the podocytes bearing the mutant variants of RhoGDI α is different from that of control podocytes. A difference here could partially explain the defective function of podocytes in vivo. We first performed a wound healing assay (**Figure 10A**). **Figure 10B** and **Figure 10C** represents the average twenty-four-hour wound healing rate of Control, RhoGDI α KD and rescued podocytes. RhoGDI α KD mouse podocytes and all three mutants (Δ D185, G173V and R120X) podocytes migrate significantly more slowly than control cells. When RhoGDI α KD podocytes were rescued with the WT RhoGDI α , their motility was partially restored (**Figure 10B**).

We repeated the experiment with control, RhoGDI α KD and RhoGDI α KD rescued with Δ D185 in two different conditions. One pool of each cell line was kept in culture in vehicle (control condition) containing media and another pool of each was treated with Rac1 inhibitor, NSC23766at 50 μ M. Cells were serum starved overnight in 0.5% FBS in RPMI prior to proceeding to the wound healing experiment. We observed an important decrease in the motility of all the mouse podocyte lines (data not shown). We also tested the migration of the same three lines but with RhoA inhibitor, C3 Transferase (C3). The result is reversed. All three- control, RhoGDI α KD and RhoGDI α KD rescued with Δ D185- migrated faster when treated with C3 than in their respective vehicle condition. Statistically speaking, C3 partially restored the motility of RhoGDI α KD and Δ D185 rescued mouse podocytes (**Figure 10D**).

3.2.2.1.3- Altered coordination in extension and retraction of RhoGDI α -defective Podocytes

The wound healing assay showed that control cells migrate faster than other podocytes cell lines. They do close a wound faster in a twenty-four-hour span. We next studied by mechanisms

of impaired cell migration of RhoGDI α -defective mouse podocytes. We were interested in the coordination in the movement of podocytes that allows them to migrate properly. Hyperactivation of Rho-GTPases may affect that coordination, leading to impaired directional movement and to a diminished net migration. We used live cell imaging and tracking to examine the coordination concept. Live control, RhoGDI α KD and Δ D185 rescued mouse podocytes were imaged for 3 hours at a 10X magnification every 10 minutes to study their motility. After the acquisition, we used Zen Imaging Software to track the itinerary of individual cells. Since 3 hours is a short amount of time to register relevant motility, we stimulated the podocytes with EGF (at 100nM) to optimize the process. We calculated the total distance (along the itinerary) and the displacement (distance between the position at time zero and at 3 hrs) of the podocytes. We expected that RhoGDI α KD and Δ D185 rescued podocytes will move as well or more than control cells but we believed that the movement will not be directional and the final displacement will be less, as compared with control cells. **Figures 11A, 11B and 11C** report the recorded trajectories of all the cells of interest. The average distance and average displacement of RhoGDI α KD and Δ D185 rescued podocytes were both reduced as compared to those of control podocytes (**Figure 11D**). Control cells migrate in average about two times more than RhoGDI α KD and Δ D185 podocytes in 3hours. The results differ from the hypothesis stating that RhoGDI α KD and Δ D185 rescued podocytes would have a defect in directional movement but not in total distance travelled: the RhoGDI α -defective cells appeared to have a generalized defect in cell movement. Therefore, we next studied the behavior of individual cells at the cell membrane level, i.e. at the membrane ruffling.

Since differentiated podocytes' membrane ruffling is important in cell motility, that membrane ruffling is dependent on the presence of the GTPase-activating protein (GAP) and considering that GAP works tightly in collaboration with other members of the GEF, GAP, GDI cycle, we hypothesized that Δ D185 cells would show altered membrane ruffling behaviour, which would be consistent with previous results showing a defect in cell migration [48]. The decreased migration could be due to a coordination problem in the ruffling functions. Accordingly we next examined the membrane dynamics of podocytes by kymograph. Kymographs give information about the spatial position of an element of interest in time on a graph. Our element of interest is the membrane ruffling in mouse podocytes' protrusions. Podocytes were transfected with mCherry-actin and stimulated with EGF. We observed the cells extending and retracting during

their migration. One to four protrusions were examined per cell. The ruffling of these protrusions was imaged every 15 seconds for 20 minutes. From our acquisitions, we used the MultipleKymograph plugin for ImageJ to generate kymographs. Even though it is difficult to assess a clear directional pattern in motility within 20 minutes, control podocytes appeared to move more directionally than RhoGDI α KD and Δ D185 podocytes (**Figure 12A**). The plugin and the instructions needed to generate kymographs for elements of interest for a given time frame can be found on http://www.embl.de/eamnet/html/body_kymograph.html. The Kymographs represent the leading position of podocytes' protrusions for a given time. The X-axis represents the position in space, the Y-axis represents the time. RhoGDI α KD podocytes were switching from extension to retraction more frequently than control podocytes did (**Figure 12B**). The Δ D185 mutant podocytes tended to have more phase switches than control podocytes but we were not able to establish a significant difference. Hence, uncoordinated actin movement at the leading edge of the cell is likely contributing to the defective motility of RhoGDI α KD and possibly of Δ D185 podocytes (clinically speaking).

3.2.2.1.4- Fluorescent Resonance Energy Transfer

In human fibroblasts, the Δ D185 mutation caused the cells to be less responsive to the RhoA activator (**Figure 5A** and **Figure 5B**). We next studied if a similar blunted response would be observed in mouse podocytes. Control and RhoGDI α KD mouse podocytes were transfected with the RhoA probe Raichu-1502 and serum starved prior to acquiring live cell images. As it was done for human fibroblasts, pictures were taken at time 0 and every 2 minutes for ten minutes after stimulation of RhoA with calpepin. The activation of RhoA, quantified as described for human fibroblasts, was significantly weaker following stimulation in RhoGDI α KD podocytes, as compared with control: average slope for control = -0,06198, STDEV = 0,052677, n = 10 cells; average slope for RhoGDI α KD = -0.02095, STDEV = 0.021778, n = 10 cells; p = 0.0185 (not shown). The results were similar to those observed in Δ D185 human fibroblasts (CNS). We speculate that the absence of functional RhoGDI α led to degradation of RhoA, leaving very little inactive RhoA to be available when we stimulate its activation [37]. The experiment was not carried on with the mutant cells as the GFP-tagged RhoGDI α transfected into the mouse podocytes interfered with FRET signals.

3.2.2.2- Consequences of RhoGDI α Mutations on Podocytes Morphology

3.2.2.2.1- Affected actin polymerization in RhoGDI α -defective Podocytes

Since the mutant RhoGDI α doesn't bind to RhoA, or at least has a much reduced capacity to do so, active RhoA is increased which is likely reflected in cells' morphology or function [7]. One way to measure the increased activity of Rho-GTPases in the morphology of cells is to compare the F-actin intensity/ G-actin intensity ratio of the different RhoGDI α -defective cell lines to that of the control cells. Filamentous actin is the polymerized form of the monomer Globular actin, and because RhoA regulates polymerization of G-actin into F-actin, we expected to witness a disruption of F/G –actin ratio parallel to an increased Rho-GTPases activity. In other words, an increase or a decrease of actin polymerization is expected in RhoGDI α -defective podocytes. We stained mouse podocytes with Phalloidin 555 and DNASE I 594 as indicated in the methods section. Even though Phalloidin555 dye and DNASE I 594 dye are close to each other in a wave length point of view, we were able to distinguish them by using two different lasers, 561 and 633 from a Confocal Microscope , LSM780 Zeiss. We repeated the experiment 5 to 6 times. Since the variability between sets of experiment was large, the F/G actin ratios were normalized to the average of the control cells in each set of experiment. RhoGDI KD as well as RhoGDI KD rescued with the mutant forms of RhoGDI α showed a lower F/G-actin ratio than control cells (**Figure 13A**). This implies that high Rho-GTPases' activity decreases F-actin levels. The rescue of RhoGDI α KD cells with WT RhoGDI α restored the F/G –actin ratio (at least partially) (**Figure 13B**).

We next conducted experiments with RhoA or Rac1 inhibitor in order to determine which Rho-GTPase was responsible for the decreased actin polymerization. Mouse podocytes (Control, RhoGDI α KD and Δ D185) were cultured in RPMI with 10% FBS and serum starved overnight prior to running the experiment. A group of each cell line was preserved in normal condition. A second group was treated overnight prior to staining and plating with the RhoA inhibitor, C3. Inhibition of RhoA did not affect the F/G –actin ratio of control and Δ D185 podocytes. However it did further reduce the F/G – actin ratio of RhoGDI α KD podocytes (**Figure 13C**).

Analogous experiments were done in the presence or absence of the Rac1 inhibitor, NSC23766. Inhibition of Rac1 restored the normal F/G –actin ratio of RhoGDI α KD podocytes rescued with Δ D185 but did not restore that ratio for RhoGDI α KD cells (**Figure 13D**).

3.2.2.2.2- Affected cell length and size of RhoGDI α -defective Podocytes

A deregulation of the Rho-GTPases' balance and the resulting alterations in actin cytoskeleton dynamics would likely affect the morphology of the cells. From then on, we next studied the morphology of podocytes. As we observed Phalloidin-stained podocytes, we noted that the RhoGDI KD and mutant rescued cells appeared shorter than control cells. To quantify this we used the ratio of the length and the width of the cells. The length was defined as the longest diameter of the cells' body whereas the width was defined as the shortest diameter of the cells' body (excluding the diameter of protrusions). **Figure 14A** shows how the measurements were taken. For irregular shape cells we measured the width at two or three different sites and then calculated the average of all the measurements that were used as the width of the cell (used on triangular shape cells for example). RhoGDI KD podocytes and all three mutant-rescued podocytes have a lower length/width ratio than control podocytes. In other words they are shorter than control podocytes or control podocytes are more elongated (**Figure 14B**).

Another morphological characteristic that appeared to be affected in KD and mutant rescued cells was the size. These cells appeared smaller than control podocytes. When the cross-sectional areas were quantified, we found out that control cells were bigger than KD and RhoGDI α mutants rescued cells (**Figure 14C**). The reduced cell size of RhoGDI KD podocytes was restored when rescued with WT RhoGDI α (**Figure 14D**).

We next examined if Rac1 hyperactivation plays a role in these morphological changes using GDI KD and Δ D185-rescued cells. The Rac1 inhibitor restored the length and cell size of Δ D185-rescued cells, but not those of KD cells (**Figure 15A** and **Figure 15B**).

3.2.2.2.3- Affected protrusion formation in RhoGDI α -defective Podocytes

Another striking change in RhoGDI α -defective podocytes was the increased amount of protrusions. In order to quantify the significance of this change, we defined two types of protrusions that we called extensions and spikes in Phalloidin-stained cells. We decided to set a

limit in the dimensions of protrusions to distinguish them from each other and from non significant fibres, artefacts and dead cell fragments. Extensions were defined as any cellular protrusions that have a length at least 40% that of their respective cell's length (i.e. longest diameter) and a width that measures 15% the width of their respective cell. A spike was defined as a protrusion that has a length measuring at least 15% the length of its respective cell and a width at the base measuring at least 10% the width of its respective cell (**Figure 16A**).

RhoGDI α -defective Podocytes having a higher Rac1 activity than control, we anticipated a higher number of extensions and spikes in those Podocytes. Using ImageJ measuring tools, we were able to count the protrusions per cell lines. **Figure 16B** is a graph showing the average number of extensions and spikes per cell line. RhoGDI α KD as well as all three RhoGDI α mutant cells showed increased number of these protrusions. Although for KD cells, the difference did not reach statistical significance. The Rac1 inhibitor did not alter the number of protrusions in control cells but reduced the number of protrusions in KD and Δ D185 to the control level (**Figure 16C**). This was the only morphological change in RhoGDI α KD mouse podocytes that was restored by Rac1 inhibition.

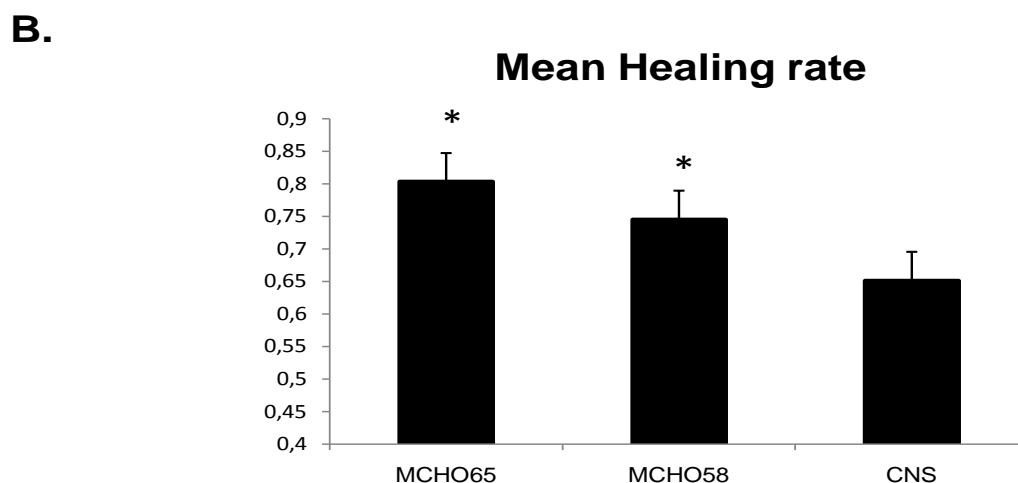
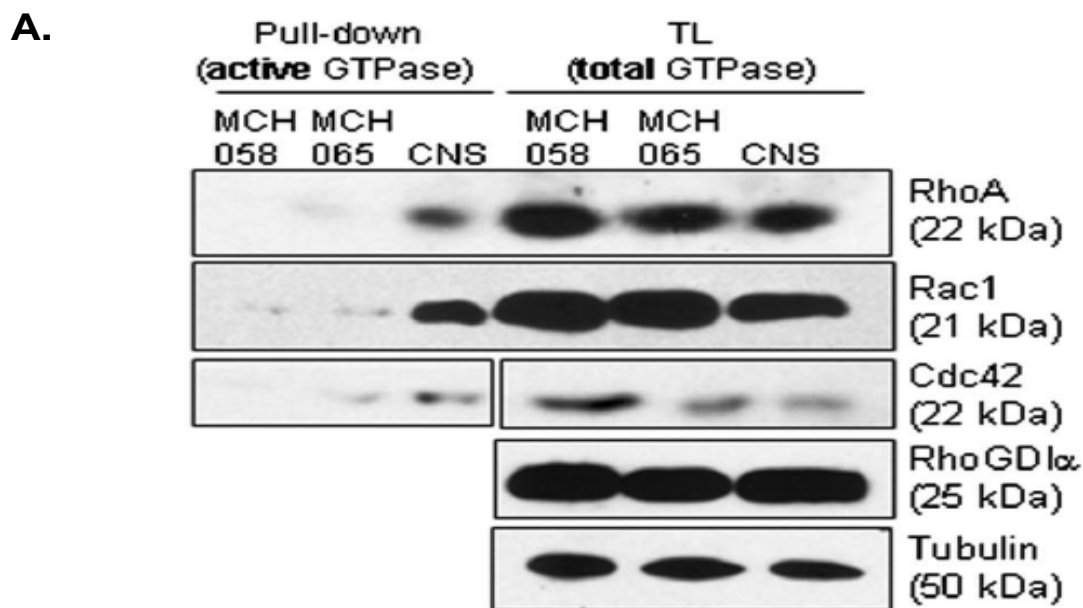


Figure 4: RhoGDI α Δ D185 mutation causes decreased efficiency of RhoGDI α that impairs cell motility.(A). On the right side of the panel we have a Western Blot showing expression level of Rho-GTPases and RhoGDI α for control (MCH065 and MCH058) and mutant (CNS) human fibroblasts. On the left is a pull-down of active forms of Rho-GTPases found at higher level in CNS. (B).This is the results of a Wound Healing assay showing that CNS human fibroblasts migrate more slowly than MCH065 and MCH058. * P = 0.001 & 0.033 respectively compared with CNS; n = 5 experiments (14 to 18 measurements).

A.

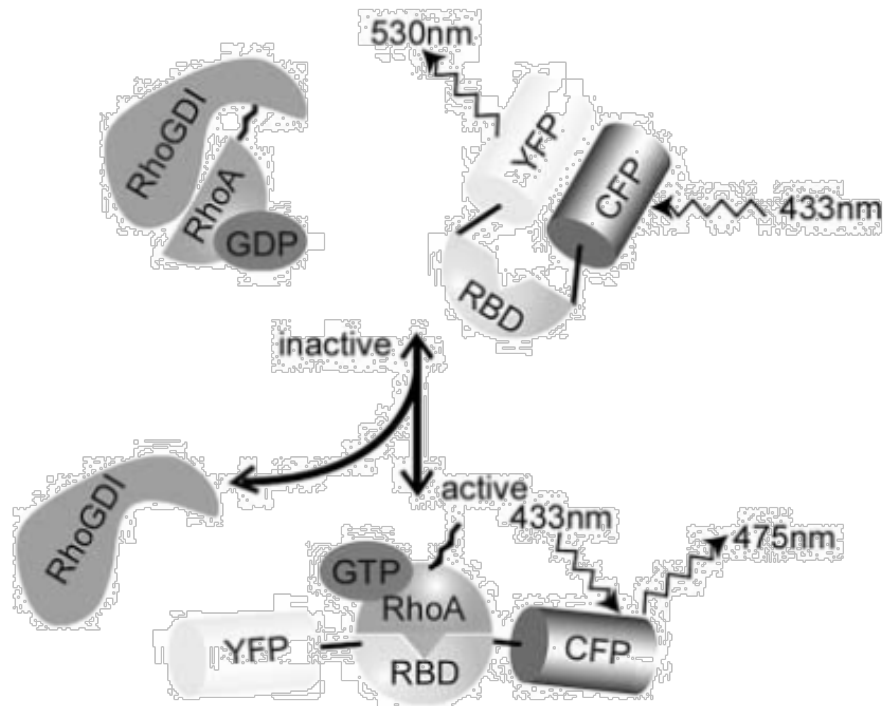


Figure 3: Spatio-temporal profile of RhoA activity by live cell imaging technique fluorescence resonance energy transfer (FRET) shows a blunted response of CNS human fibroblasts upon stimulation by calpeptin. (A). RhoA probe Raichu-1502 binds to the active form of RhoA (released from RhoGDI α to convert into GTP form) and reduces the FRET signals. CFP and YFP are initially in contact for emission-reception. Activated RhoA binds and separates them. Therefore, low FRET signal corresponds to high RhoA activity [2].

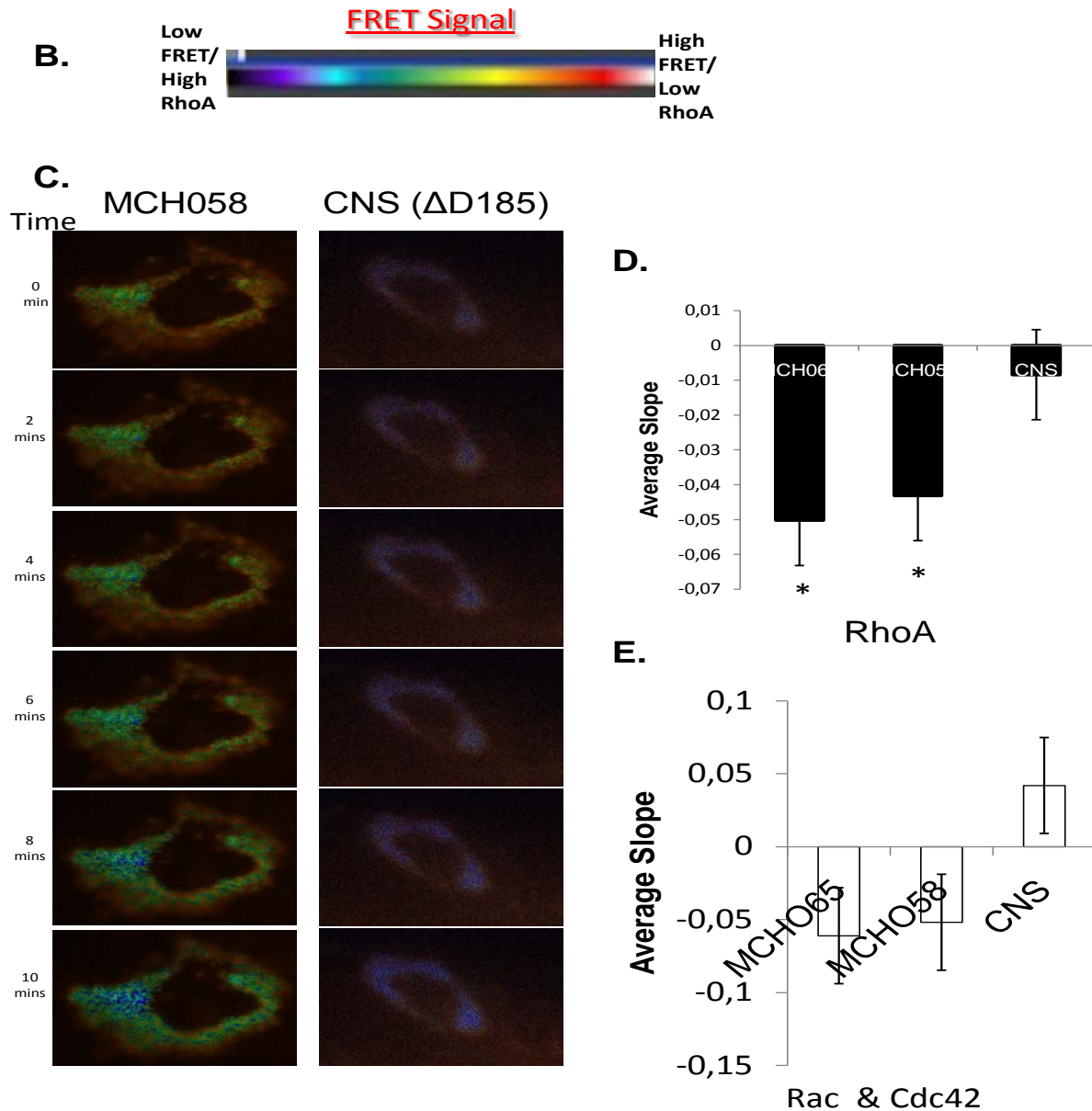


Figure 5: Spatio-temporal profile of RhoA activity by live cell imaging technique fluorescence resonance energy transfer (FRET) shows a blunted response of CNS human fibroblasts upon stimulation by calpeptin- Cont'd. (B). The FRET bar shows the inverse relationship between FRET signal and RhoA activity. (C). MCH058 responded better to calpeptin (orange to blue) than CNS (blue to purple) shown by the change in intensity in FRET signal. (D). Mean change in intensity of FRET signal for RhoA per human fibroblast line where «*» means a significant difference with respect to CNS ($p < 0.05$; $n = 10$ to 11 cells). (E). Recapitulation of (D) but with Rac and Cdc42.

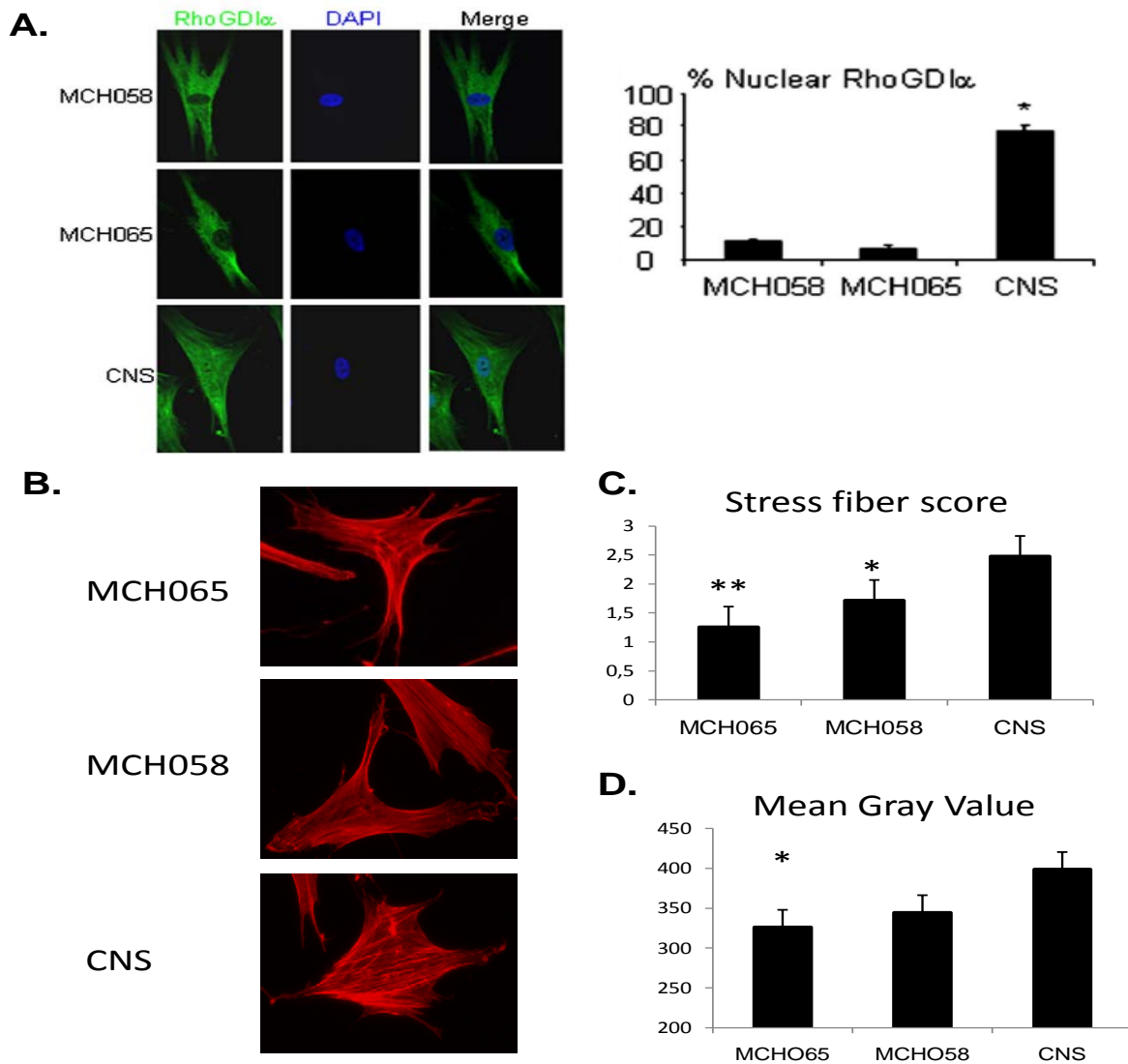


Figure 6: Mutant RhoGDI α Δ D185 is mislocalized in the nucleus and increases F-actin levels in human fibroblasts. (A).RhoGDI α is normally localized in the cytosol of cells. Here in CNS fibroblasts, RhoGDI α is also found in the nucleus. The graph shows the percentage of cells in which RhoGDI α is found in the nucleus. The «*» here indicates a significant difference between CNS and both MCH065 & MCH058. $P < 0.01$, $n = 4$ experiments with 40 to 56 cell counts [1]. (B). Representative images of stress fibre level in human fibroblasts. (C). The average SSS per human fibroblast cell line. A «*» or «**» mark significant differences in SSS with respect to CNS. * $P < 0.05$, ** $P < 0.001$ $n = 3-4$ experiments; cell counts 40-56. (D). The average MGW shows a similar trend to SSS. A «*» indicates a significant difference with respect to CNS. * $P < 0.05$, $n = 3-4$ experiments, cell counts 40-56

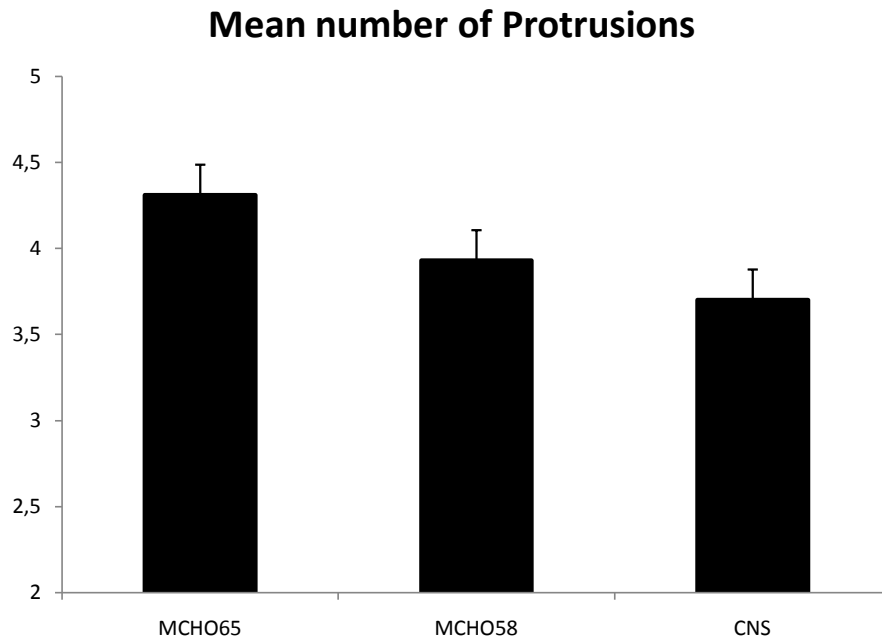


Figure7: Mutation of RhoGDI α Δ D185 decreases cellular protrusions in human fibroblasts. This graph represents the average number of protrusions per human fibroblasts cell lines from three sets of experiments (40 cells per cell line). The trend shows a smaller number of protrusions in CNS human fibroblasts than in both controls.

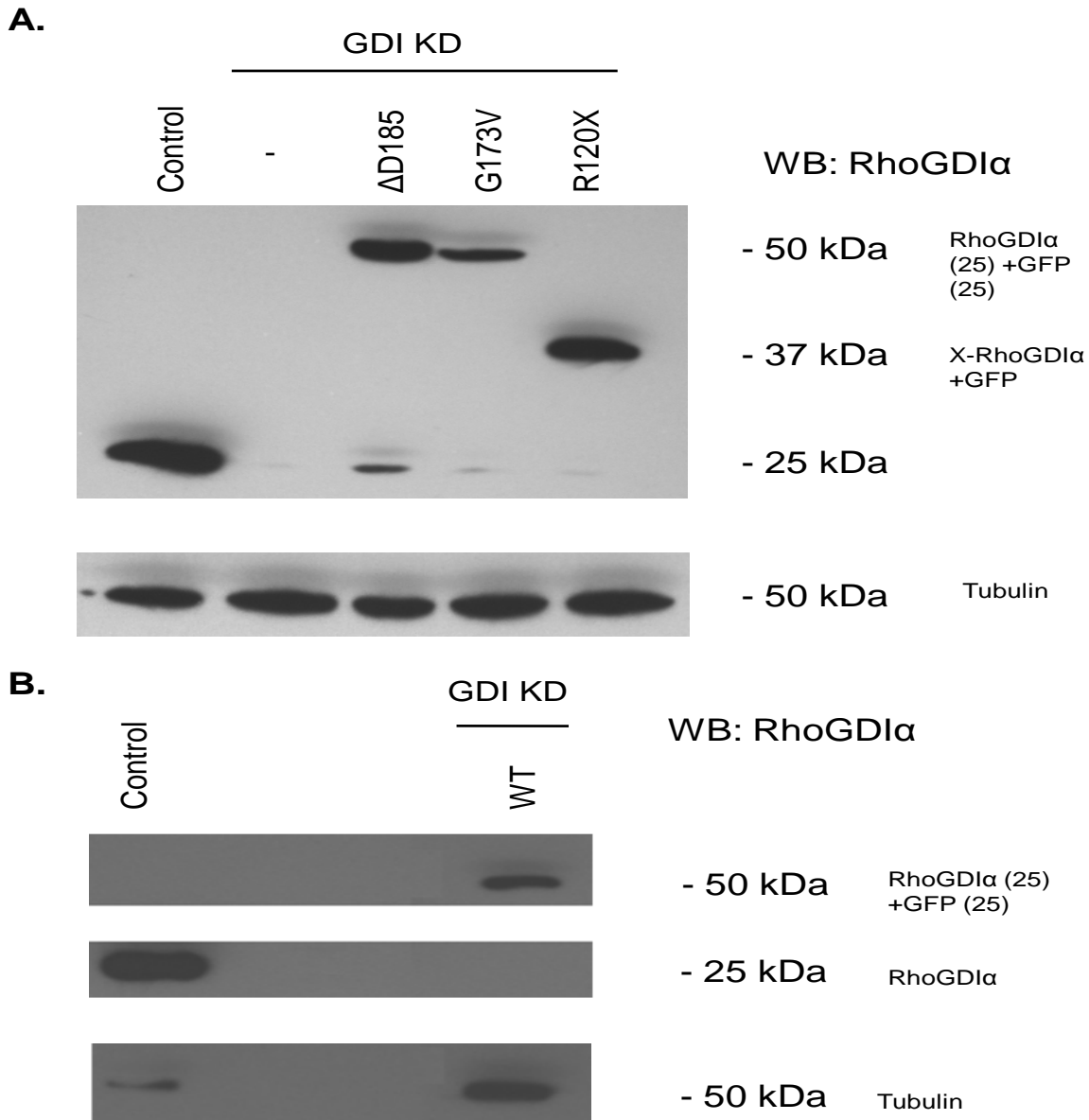
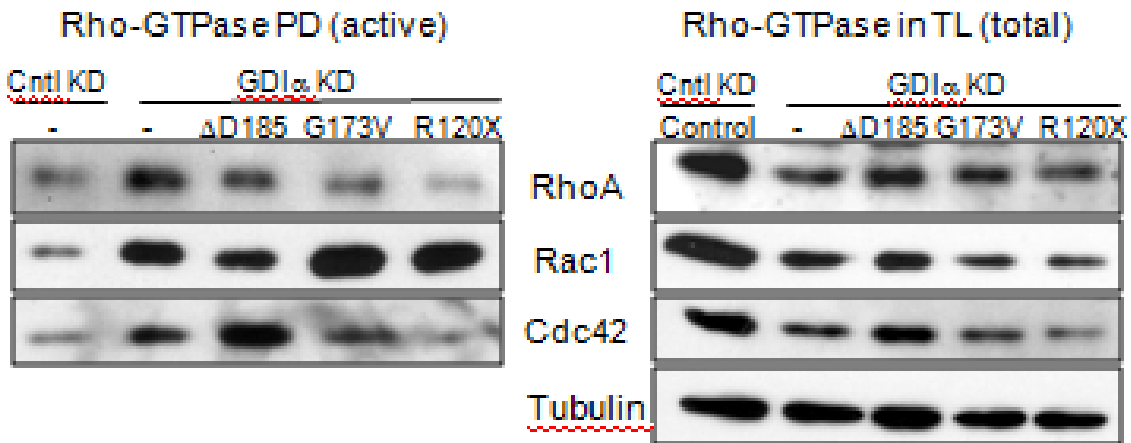


Figure 8: Establishment of the KD cells and rescue with mutants and Wild Type. (A) Here we have a western blot showing the expression of RhoGDI α in mouse podocytes. At 25 kDa we have the endogenous form of RhoGDI α in control podocytes. Other cells were RhoGDI α KD. A KD line was kept as is and three lines were rescued with GFP-tagged mutants RhoGDI α (Δ D185, G173V, R120X from left to right) or wild type (WT) visible at 50kDa (RhoGDI α + GFP). At 37kDa is the truncated R120X RhoGDI α . The weak bands at 25kDa are degradation products of GFP-tagged RhoGDI α . (B) Here we have a western blot showing expression of endogenous RhoGDI α (Control) and GFP-tagged RhoGDI α KD rescued with RhoGDI α .

A.



B.

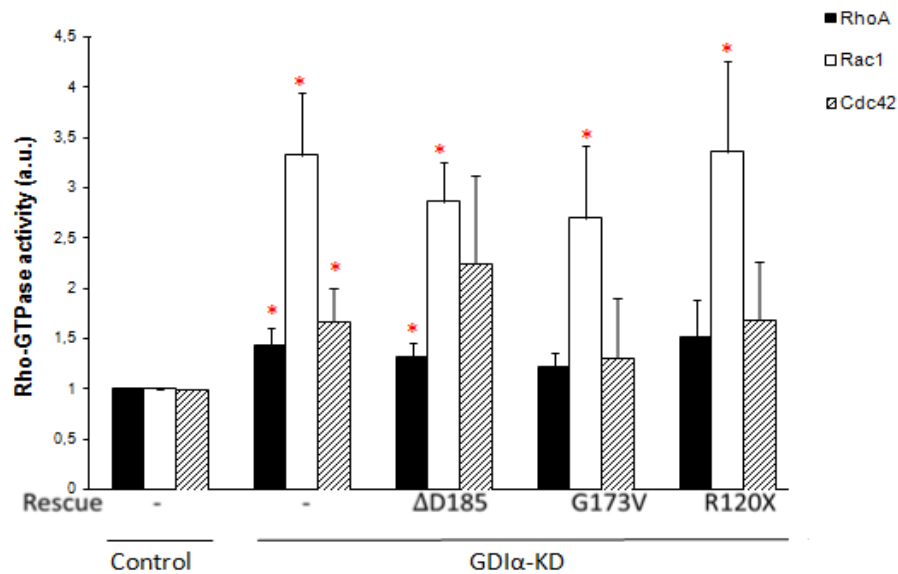


Figure 9: RhoA, Rac1 and Cdc42 Activities are Increased in RhoGDI KD and Mutants Podocytes Compared to Control Cells.(A). RhoA, Rac1 and Cdc42 activities detected by pull-down assay were generally higher in RhoGDI α KD podocytes and the three mutant-carrying podocytes. (B). This graph is the quantification of the pull-down assay. A «*» indicates a significant difference of respective Rho-GTPases levels compared to control. p<0.05, n=3-6.

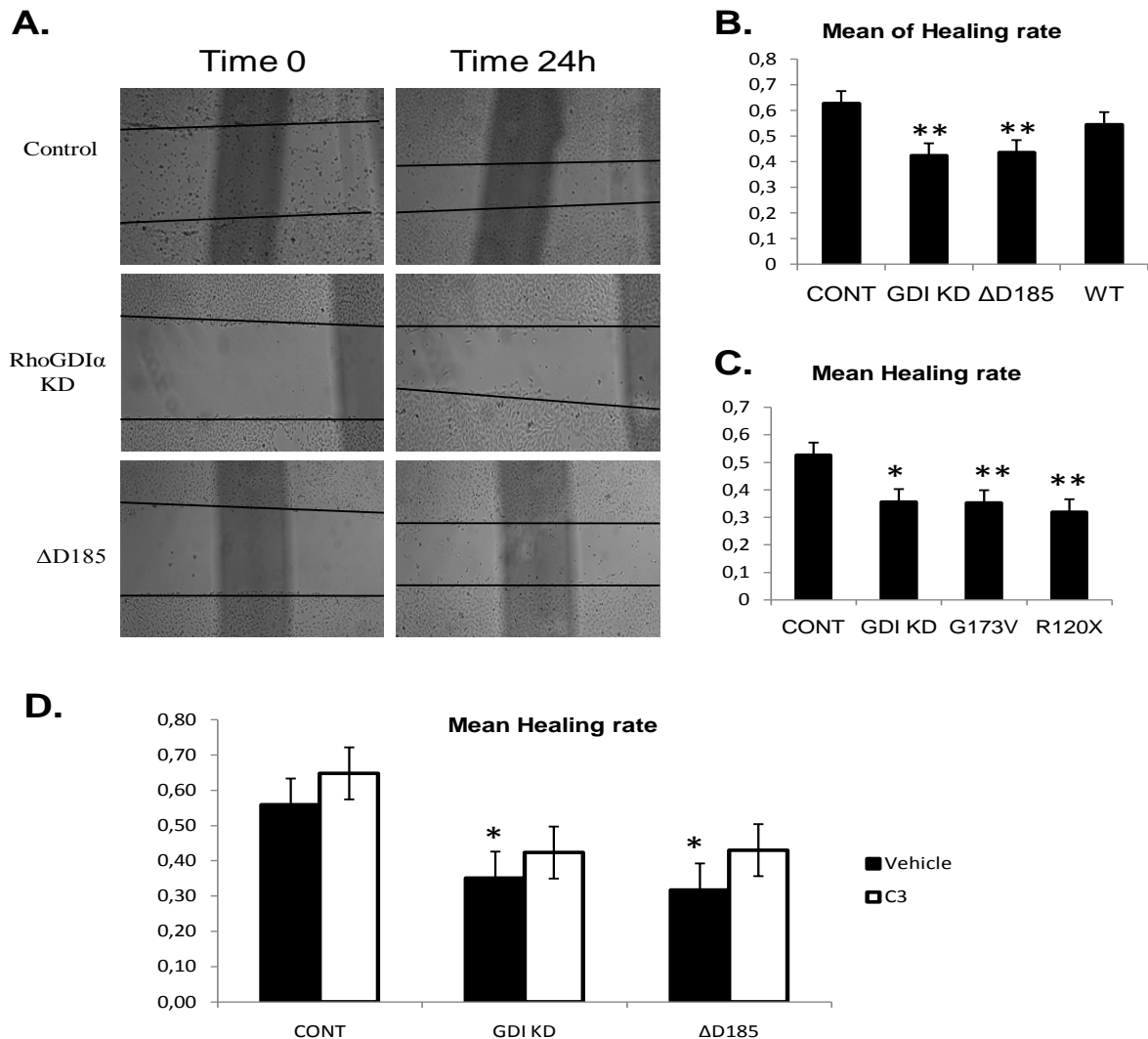


Figure 10: The Δ D185, G173V & R120XRhoGDI α cause impaired migration of podocytes. (A). Here we have the wound surface area of different mouse podocyte lines. Panels on the left show the wound surface area at time 0. The right panels show the wound surface area after 24 hours. (B). RhoGDI α KD and Δ D185 podocytes migrate more slowly than control cells. **P<0.001 compared to control; n= 8 experiments. (C). The graph represents the mean healing rate in 24h of RhoGDI α KD, G173V & R120X compared to control. *P=0.002; **p<0.001; n=4 experiments (D) Here we have the mean healing rate of podocytes with and without RhoA inhibitor, C3 (0.1 μ M) overnight. *P<0.05, n=5 experiments.

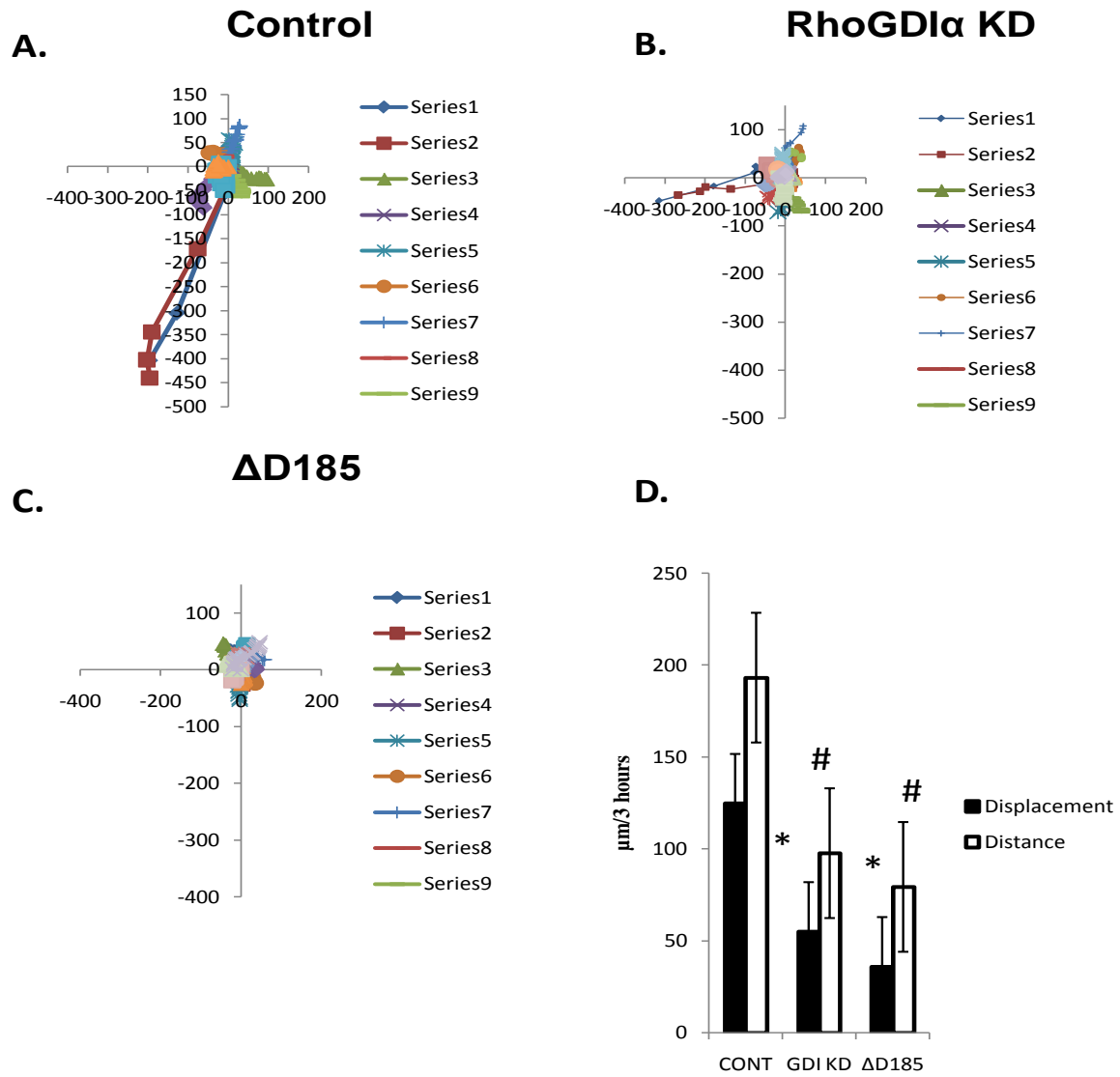
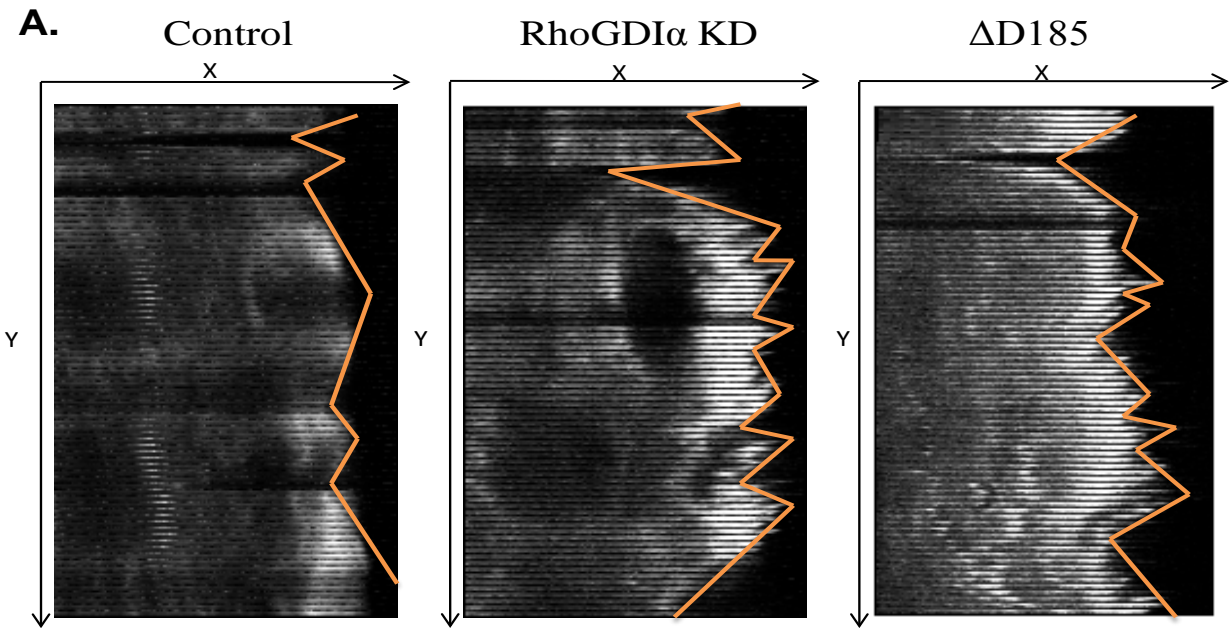


Figure 11: The Δ D185 mutant RhoGDI α provokes a decrease in net motility of podocytes.

Cells were stimulated with EGF (at 100nM)(A). Movement of control podocytes tracked in $\mu\text{m}/3$ hours. (B). Movement of RhoGDI α KD podocytes tracked in $\mu\text{m}/3$ hours. (C). Movement of Δ D185 podocytes tracked in $\mu\text{m}/3$ hours. (D). Graph of the average displacement and average distance of migration of podocytes. The «*» indicates a significant difference (at $p < 0.05$) of average displacement of RhoGDI α -defective podocytes with respect to control. $n = 12$ to 27 cells from 3 experiments A «#» marks a significant difference (at $p < 0.05$) of average total distance covered in podocyte migration respective to control. $n = 3$ experiments.



B.

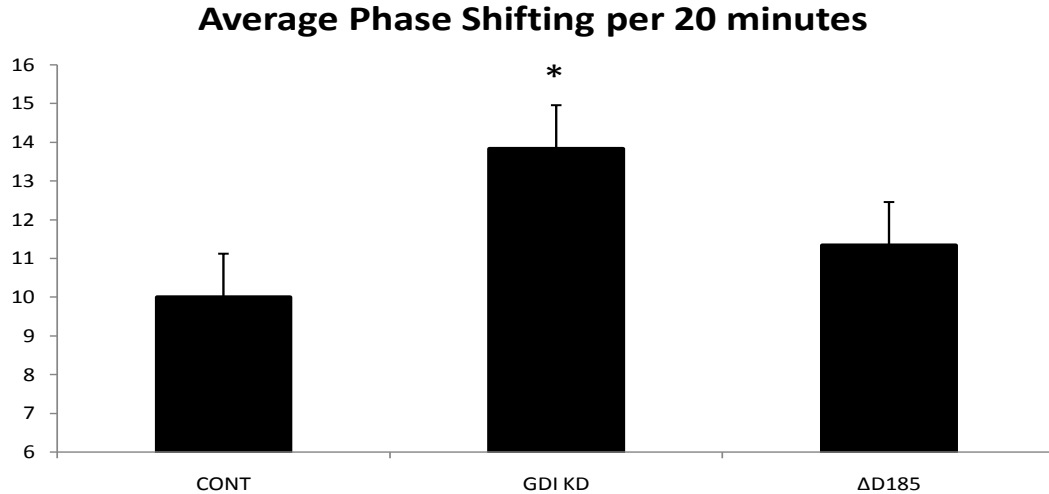


Figure 12: RhoGDI α knockdown leads to augmented extension-retraction cycles of membrane ruffling in podocytes (A). Here we have the kymographs of membrane ruffling of control, RhoGDI α KD and Δ 185 podocytes over 20 minutes. The orange lines mark how were the phase shifting counted (B). The graph represents the average phase switches (extension to retraction to extension) per podocyte lines over 20 minutes. The «*» indicates a significant difference (at $p < 0.05$) when compared to control; $n = 3$ experiments, cells count 3 to 4 cells: 1 to 4 ruffling were analysed per cell.

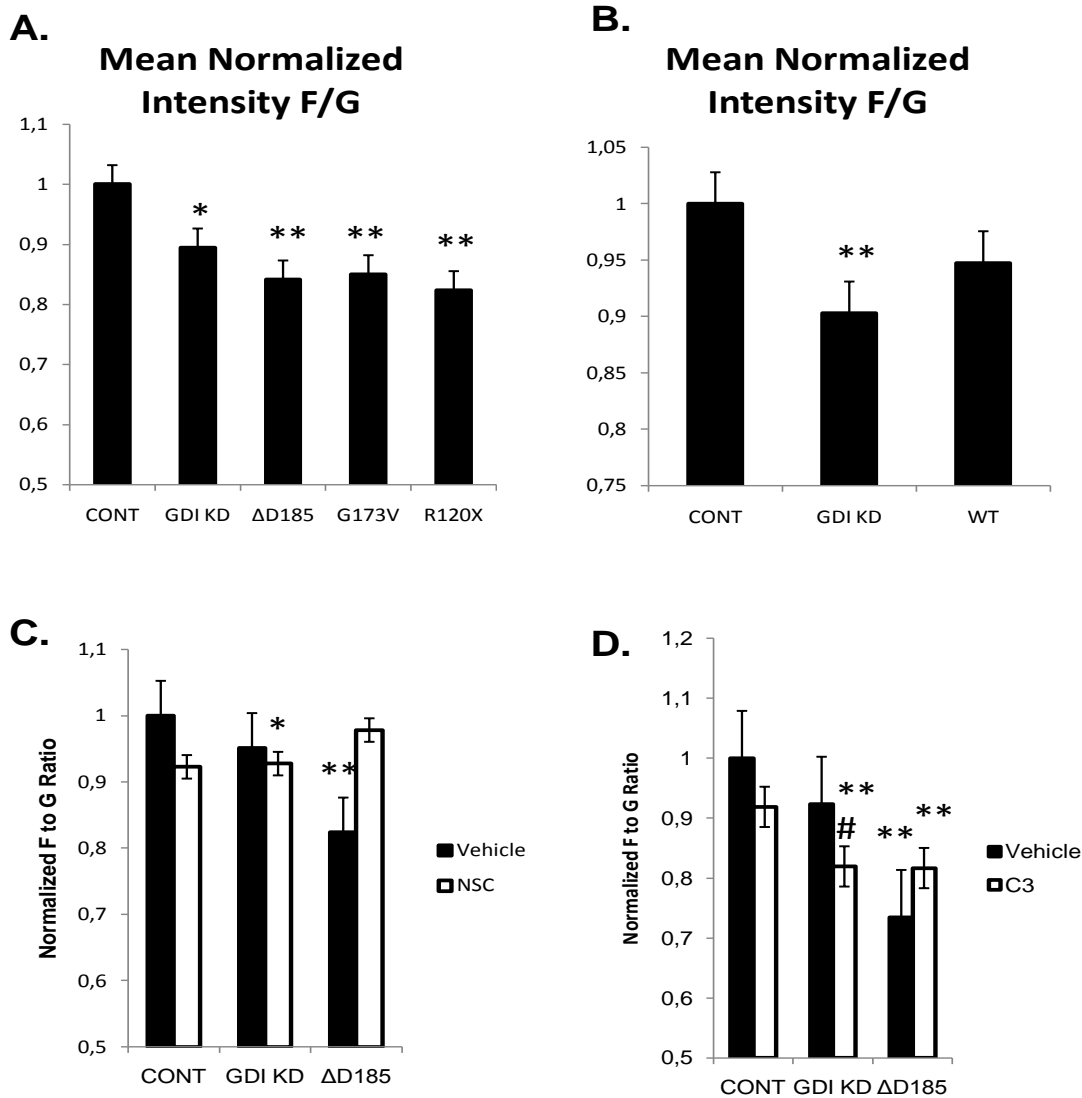


Figure 13: Mutant RhoGDI α s cause reduction of F/G-actin Ratio. The «*» and «**» marks a significant difference compared to control (* $p < 0.05$; ** $p < 0.001$)). (A). Here we have the average normalized F-actin to G-actin staining intensity ratio of control and RhoGDI α -defective mouse podocytes (values normalized to Control of each set of experiments). $n = 60$ to 126 cells from 7 experiments. (B). A graph showing a partial restoration of F/G-actin ratio of RhoGDI α KD podocyte transfected with WT RhoGDI α . $n = 56$ - 82 cells from 4 experiments (C). Average F/G-actin ratio of podocytes with and without the Rac1 inhibitor (NSC23766, $50\mu\text{M}$). $n = 41$ to 52 cells from 3 experiments (D). Average F/G-actin ratio of podocytes with and without the RhoA inhibitor (C3, at $0.1\mu\text{M}$ overnight). The «#» marks significant difference within cells lines with and without C3. $n = 46$ to 98 cells from 4 experiments

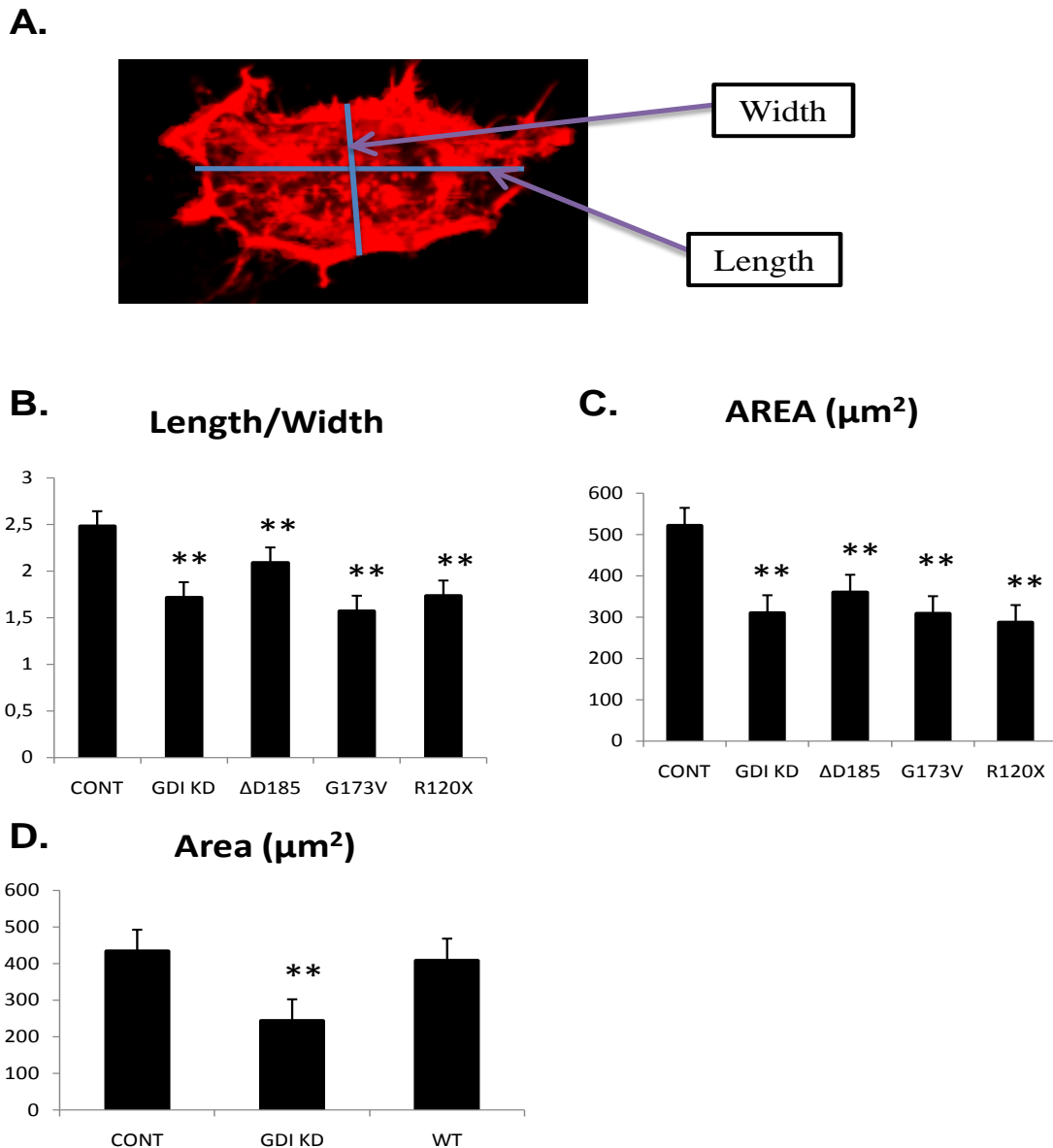


Figure 14: Mutations of RhoGDI α shorten podocytes and reduce their surface area. A «*» and «**» represent a significant difference compared to control (* $p < 0.05$ and ** $p < 0.001$). (A). Measurement of the length to width ratio. (B). Average length to width ratio of podocytes. N= 40 to 74 cells from 4 experiments (C). Graphic representation of control and RhoGDI α -defective podocytes' average surface area. N=40 to 74 cells from 4 experiments (D). A partial restoration of RhoGDI α KD podocytes' size after transfection with WT RhoGDI α . N=55 to 81 cells from 4 experiments.

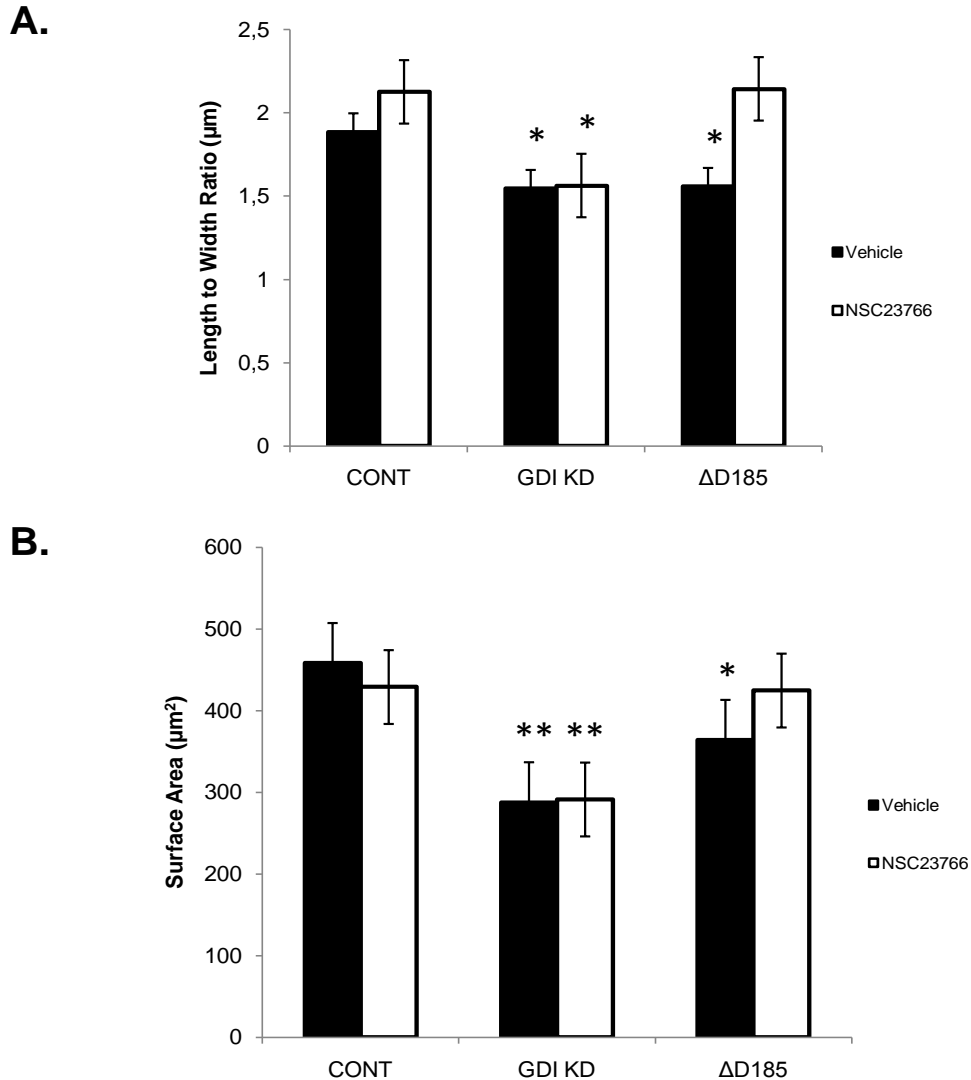


Figure 15: Rac1 Inhibitor restores the length/width ratio and size of Δ D185 Podocytes. The «*» and «**» indicate a significant difference (at * $p < 0.05$ and ** at $p < 0.001$) compared to control with vehicle. (A). The graph represents the average length/width ratio of control, RhoGDI α KD and Δ D185 podocytes. The cell lines are divided in two groups: without and with treatment of Rac1 inhibitor (NSC23766, at 50 μ M). N=57 to 88 cells from 6 experiments (B). The mean podocyte surface area per podocyte lines is represented in this graph when treated or not with Rac1 inhibitor (NSC23766, at 50 μ M) as in A. N= 56 to 83 cells from 4 experiments

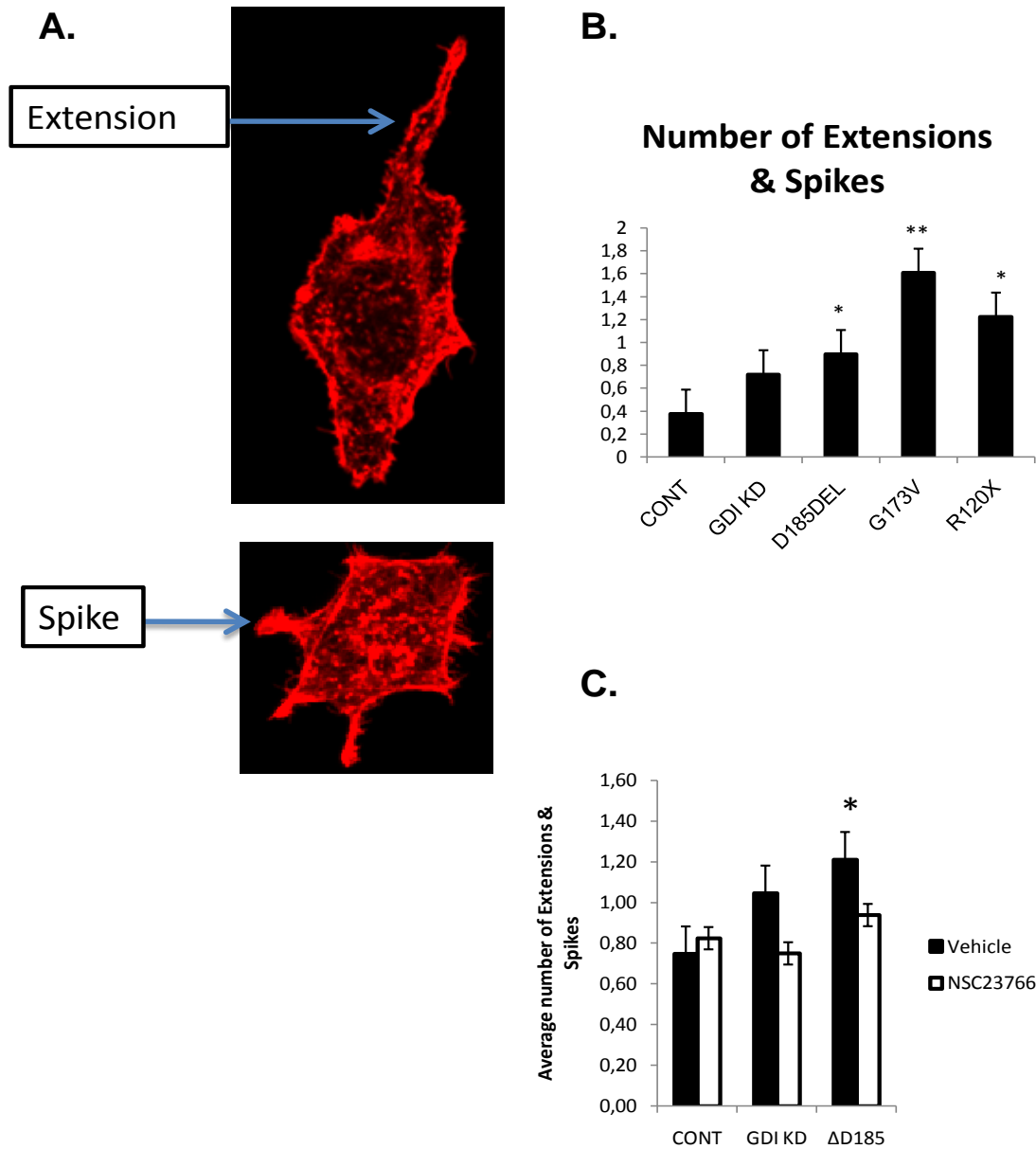


Figure 16: Mutant RhoGDI α s increase cellular protrusions. The «*» and «**» indicates a significant difference (at * $p < 0.05$ and ** $p < 0.001$) compared to control in vehicle. (A). Representation of extensions and spikes (see text for details). (B). Here we have the average number of extensions and spikes per podocyte line. N=40 to 74 cells from 4 experiments (C). Here we have the average number of extensions and spikes for control, RhoGDI α KD and Δ D185 mouse podocytes with or without Rac1 inhibitor (NSC23766, at 50 μ M).

Chapter 4: Discussion

4.1- Human fibroblasts

The mutant human fibroblast line (CNS) had a lower twenty four-hour migration rate than both control fibroblasts, MCH065 and MCH058.

We used SSS and MGV for human fibroblasts to measure the actin polymerization. The Δ D185 mutation in fibroblasts increased the polymerization of actin as detected by an increased in stress fibres and intensity of Phalloidin staining.

As for the cell size, the Δ D185 fibroblasts seemed to be larger than control fibroblasts (though results were not significant) [1].

In human fibroblasts, Δ D185 mutation tends to decrease the amount of extensions (but there was not a significant difference).

4.2- Mouse podocytes

RhoGDI α KD mouse podocytes rescued with Δ D185, G173V and R120X behaved similarly to RhoGDI α KD mouse podocytes: they all migrated more slowly than control mouse podocytes.

The method used to measure the actin polymerization for mouse podocytes was the F/G-actin ratio. The Δ D185 mutation in podocytes, as well as the other mutations (G173V and R120X) showed a decrease in actin polymerization with respect to control.

When it comes to the cell size, the Δ D185, G173V and R120X podocytes were smaller than control cells. This follows a similar trend to that of RhoGDI α KD podocytes when we compared them to control, they were significantly smaller.

What we noted about the protrusions observed in mouse podocytes is that the RhoGDI α mutants significantly increased their number.

4.2.1- Podocytes' motility

Cell motility is mainly governed by the regulation of the microtubules and the actin cytoskeleton. Rho-GTPases are critical in the management of the actin dynamics. If their activity is not properly regulated, cell motility (including cell migration) will be altered. A defect in podocytes' motility is generally what is observed when these cells are affected to an extent that proteinuria is resulting [49, 50]. An increase in podocyte motility is associated with increased proteinuria parallel to a high activity of RhoA and Rac1 [43, 50]. Mele et al. reported a less effective wound healing of podocytes lacking Myo1E, leading to protein loss in urine [11]. In our study we reported a decrease in RhoGDI α -defective podocytes' migration in two different mouse podocyte lines (**Figure 4B and Figure 10**) [1]. We discovered that inhibition of the hyperactivated RhoA can restore to a certain extent the migration of podocytes in which Rac1 and Cdc42 are also hyperactivated. We obtained a totally different result when Rac1, and not RhoA, was inhibited. Cells barely migrated in a twenty-four-hour span. The partial restoration of migration with RhoA inhibition, and the significant decrease in migration with Rac1 inhibition suggest that hyperactivation of RhoA has the ability to inhibit the migration, . Rac1 activity is required for migration. Nevertheless, inhibition of RhoA wasn't enough to fully restore the cell motility. This could be due to the fact that Rac1 might have reached a level that starts to be unhealthy for the cell to exhibit normal motility. RhoA is also known to play an important role in cell migration and the absence or a too low level of RhoA lead to proteinuria [50, 51]. Inhibiting RhoA can help improving migration of cell if RhoA is hyperactivated but it is not sufficient for a normal motility. There must be an optimal level of RhoA activity and Rac1 activity for an optimal motility. A high RhoA activity could cause an increase in cell motility until it reaches a point where cell motility is decreased. In both cases, the result leads to proteinuria.

4.2.2- Differential hyper-activation of RhoA, Rac1 and Cdc42 by RhoGDI α KD or mutant RhoGDI α s

Mutant mouse podocytes had a higher level of active RhoA and Rac1 as compared with control podocytes. In contrast, Cdc42 was the least consistently hyperactivated which was why experiments were carried on with the examination of RhoA and Rac1 more particularly. This

does not infer that Cdc42 is not relevant to our case. It is noteworthy that all three Rho-GTPases were consistently significantly hyperactivated in RhoGDI α KD with respect to control podocytes, while mutant RhoGDI α s conferred variable Rho-GTPase activation.

Another striking finding was the ability to restore a variety of altered podocyte morphological characteristics in Δ D185 mutants by using Rac1 inhibitor. This does not apply to RhoGDI α KD podocytes. Four morphological features, namely the F/G-actin ratio, the length/width ratio, the cell size and the number of protrusions were all affected in both RhoGDI α KD mouse podocytes and Δ D185 mutant-carrying mouse podocytes and the affections followed the same trend for both RhoGDI α -defective podocyte lines. The Rac1 inhibition reversed changes only in Δ D185 cells except for the number of protrusions, where the reversal was observed in both KD and Δ D185 cells. In other words, the increase in number of cell protrusions was more sensitive to Rac1 inhibitor in RhoGDI α KD, as compared with other morphological changes.

All these findings including: generally higher Rac1, RhoA and Cdc42 in RhoGDI α KD podocytes than in other lines; the inability of the Rac1 inhibitor to restore normal morphology in RhoGDI α KD contrarily to Δ D185 mutants (for F/G-actin ratio, length/width ratio, and cell size); the efficiency of the Rac1 inhibitor to restore the extensions and spikes numbers on RhoGDI α KD mouse podocytes can be explained as follow:

- Mutant RhoGDI α s could have a partial affinity for Rho-GTPases explaining the lower activity of RhoA, Rac1 and Cdc42, as compared with the activity levels in KD cells.
- F/G-actin ratio, length/width ratio, and cell size are morphological characteristics that depend more on the active RhoA/active Rac1 (aRhoA/aRac1) ratio than on the absolute activity of each. It is established that Rac1 can affect RhoA and RhoA can also have an influence on Rac1 activity (often antagonistic). Rac1 activity could have reached a level so high in RhoGDI α KD mouse podocytes that using NSC23766 (at 50 μ M) was not sufficient to lower its level to normalize the aRhoA/aRac1 ratio. In Δ D185, aRac1 is initially high too, but not as high as in RhoGDI α KD cells, explaining why the F/G – actin ratio, the length/width ratio, and the cell size were restored on Rac1 inhibition.

Using a higher concentration of Rac1 inhibitor in RhoGDI α KD cells could be helpful to verify that theory since the half maximal inhibitory concentration of NSC23766 (IC50) is $\sim 50\mu\text{M}$, which is the concentration we used [52]. The concentration has to be adapted to the cell types, but a window of $50\mu\text{M}$ to $200\mu\text{M}$ has been used [53]. The RhoA inhibitor did not change the F/G-actin ratio in control and ΔD185 podocytes but decreased it significantly in RhoGDI α KD podocytes which is consistent with the hypothesis of the critical role of the aRhoA/aRac1 ratio in actin polymerization: Rac1 was initially much higher in RhoGDI α KD cells. Decreasing RhoA activity would most likely decrease the aRhoA/aRac1 ratio (**Figure 17**). In terms of Rho-GTPases quantification comparison, the clinical interpretation is more important than the statistical interpretation (as usual).

- The number of extensions and spikes appears to be regulated only by the activity of Rac1 (among the studied Rho-GTPases). It is likely that there are certain thresholds in the level of Rac1 activity that determine the amount of protrusions. If the relatively high Rac1 activity is required for the formation of cell protrusions, a small decrease in Rac1 activity in RhoGDI α KD and ΔD185 cells could be enough to decrease the number of protrusions to the control level.

Initially, mutant RhoGDI α -carrying cells appeared to behave similarly to RhoGDI α KD cells. They have certain alterations to their morphology with respect to control cells. Despite all these defects, ΔD185 mutant cells respond to Rac1 inhibitor treatment, contrarily to RhoGDI α KD cells. This put the emphasis on the difference in Rho-GTPases hyperactivity levels in RhoGDI α KD cells compared to mutant RhoGDI α cells. The ΔD185 mutation might not cause a total loss of function of RhoGDI α : RhoGDI α mutant may still have a certain affinity for Rho-GTPases, particularly Rac1. This partial affinity can be tested with a co-immunoprecipitation of Rho-GTPases and RhoGDI α followed by Western blot in mouse podocytes carrying the mutants.

4.3- Parallel with human fibroblasts and mouse podocytes

It appears that RhoGDI α mutants affect cells differently depending on the nature or the type of the cells. It might be due to the fact that the aRhoA/aRac1 ratio impacts fibroblasts and podocytes differently. In other words, aRhoA might have a stronger impact on aRac1 in fibroblasts than it has in podocytes. We could verify this with the use of RhoA and Rac1 inhibitors in human fibroblasts.

Beside the reversed trends in human fibroblasts compared to mouse podocytes, it is important to note that, for all the parameters we measured, RhoGDI α mutants always had higher or lower values than controls. These values were never intermediate. For human fibroblast, where two control lines were used, CNS values, independently of significance, were never between both control lines. They were either above or below. In mouse podocytes, all three RhoGDI α mutants showed either higher or lower values than control. If one mutant had a higher value than control, all the mutants followed the same trend.

4.4- Parallel with Pull-down and FRET signal

The pull-down showed a lower level of total RhoA in mutant-carrying Δ D185 human fibroblasts but a higher level of active RhoA when compared to both control cells. This should be translated to a low baseline FRET activity (equivalent to a high RhoA activity). Even though the CNS fibroblasts showed a blunted response to calpeptin, the FRET intensity signal at time 0 did not show a significant difference as compared with both control MCH065 and MCH058 fibroblasts lines. This could be explained by the large variability among cells and the small numbers of cells studied due to the low transfection efficiency. FRET is an excellent method to detect a spatio-temporal profile of Rho-GTPase activity and is a good quantitative method when comparing the same cell over a period of time but might not be sensitive enough to compare absolute activities among different cells.

4.5- Future Directions

There always are differences in what happens in vivo and in vitro. Testing the impacts of the RhoGDI α mutations in vivo should be the next step. We should study the phenotype in mice in which we will introduce the mutant forms of RhoGDI α using a knock-in technology- knock-in construct to the delivery of heterozygous mice. These mice will be interbred to generate homozygous knock-in mice to mimic our CNS patient conditions.

Assuming that our predictions are accurately similar to what was observed in vitro, Rac1 inhibitor, NSC23766, will be used to restore normal phenotypes in affected mice.

Depending on our findings, we should plan for mutation screening in patients with congenital nephrotic syndrome and Focal segmental glomerulosclerosis (FSGS). We would determine if patients with CNS have sequence variants within the gene *ARHGDI1A*. We will also examine if other genes are pertinent to the Rac1 pathway. This new study would be done also with children with FSGS.

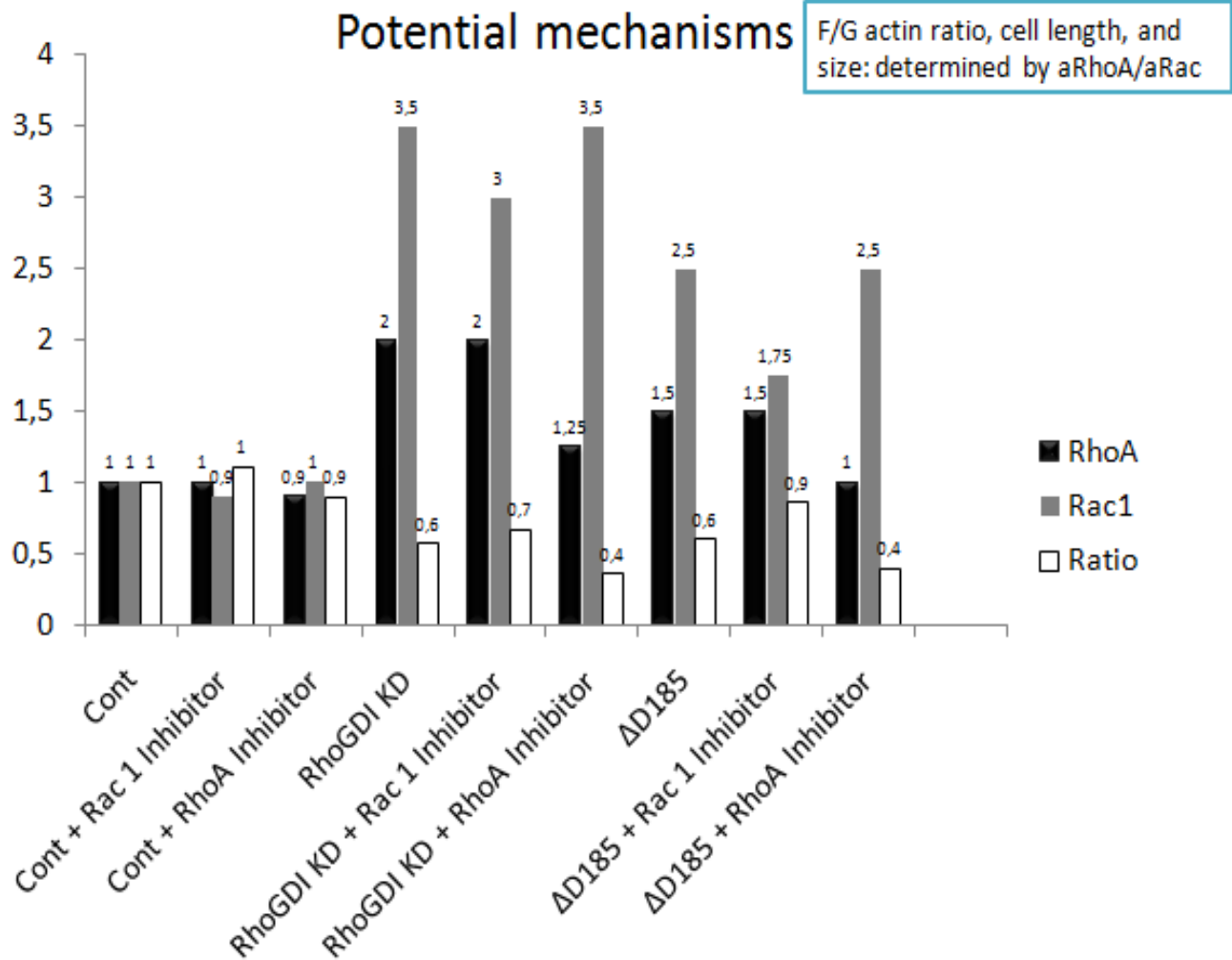


Figure 17: A potential mechanism explaining the restoration of the F/G–actin ratio, length/width ratio and surface area of Δ D185 but not of RhoGDI α KD podocytes by the **Rac1 inhibitor**. F/G – actin ratio, length/width ratio and size of podocytes appear to be governed by the ratio of active RhoA to active Rac1 (aRhoA/aRac1). Black bars represent theoretical arbitrary levels of RhoA, gray bars are for Rac1 levels and the white bars are the ratio between aRhoA and aRac1. The closer to 1 is the ratio the more the cells approach control cell standards. The levels of aRhoA and Rac1 are not solid numbers, they are based on thresholds that determine the influence that one has on the other.

Chapter 5: Summary and Conclusion

5.1- Overall Summary

1. RhoGDI α KD and mutant (Δ D185, G173V, R120X) podocytes showed hyperactivation of Rac1. RhoGDI α KD and Δ D185 showed hyperactivation of RhoA but the degree of hyperactivation was less than that of Rac1.
2. RhoGDI α KD podocytes showed a blunted response to the RhoA activator, calpeptin. CNS human fibroblasts also had a blunted response to calpeptin compared to both controls MCH065 and MCH058. This is consistent with the initially observed hyperactivity of RhoA and the decreased amounts of total RhoA.
3. RhoGDI α KD and mutant (Δ D185, G173V, R120X) podocytes migrated more slowly than control cells. The human fibroblasts CNS as well showed similar behavior compared to controls. The migration of the RhoGDI α -defective podocytes was partially restored by RhoA inhibitor (in mouse podocytes).
4. RhoGDI α KD and Δ D185 podocytes showed more phase switching (extension and retraction of protrusions), as compared with control cells. This likely translates to a defective coordination in podocytes motility.
5. RhoGDI α KD and mutant (Δ D185, G173V, R120X) podocytes had a significantly lower F/G-actin ratio than control podocytes. They were also shorter, smaller and had more protrusions than control podocytes.
6. The morphological characteristics of Δ D185 mutant podocytes were reversed by the Rac1 inhibitor (NSC23766) but not by the RhoA inhibitor (C3 transferase). In contrast, these morphological characteristics in RhoGDI α KD podocytes were not reversed by the Rac1 inhibitor. The only observed morphological feature that was restored for RhoGDI α KD

podocytes was the number of cellular extensions (that decreased to the control level on administration of Rac1 inhibitor).

5.2- The findings and Nephrotic Syndrome

- The raw theory

The dynamic control of the actin cytoskeleton is essential to maintain the shape and movement of the foot processes and to maintain cell–cell contacts. A basal level of RhoA plays a significant role in maintaining podocyte structure

Actin plays significant roles in coordinating cell shape. An unbalanced level of RhoA and Rac1 affects the shape of podocytes, explaining the elongation and size alteration of podocytes.

- The translation to Nephrotic Syndrome:

Three mutations of RhoGDI α , namely Δ D185, G173V and R120X have been reported in cases with nephrotic syndrome. These mutations lead to an increase in RhoA and Rac1 levels in the cells expressing them.

An abnormally high level of RhoA impaired podocytes motility (i.e. has reduced their migration and caused the deregulation of movement coordination). It is likely that this has impaired podocytes' migration during glomerular development and reduced podocyte foot processes' ability to adjust to filtration tumult.

An abnormally high level of Rac1 has decreased podocytes actin polymerization, shortened their length and reduced their surface area. These defects could be at the origin of gaps between podocytes in the glomerulus, allowing protein passage. In addition to that, hyperactivation of Rac1 could have increased the amount of extensions and spikes that confers aberrant foot processes.

The deregulation of RhoA and Rac1 balance would likely affect podocytes of the affected patients critically and would trigger proteinuria and instigate congenital nephrotic syndrome (**Figure 16**).

Conclusion

The control of the actin cytoskeleton is essential for the morphology and function of podocytes.

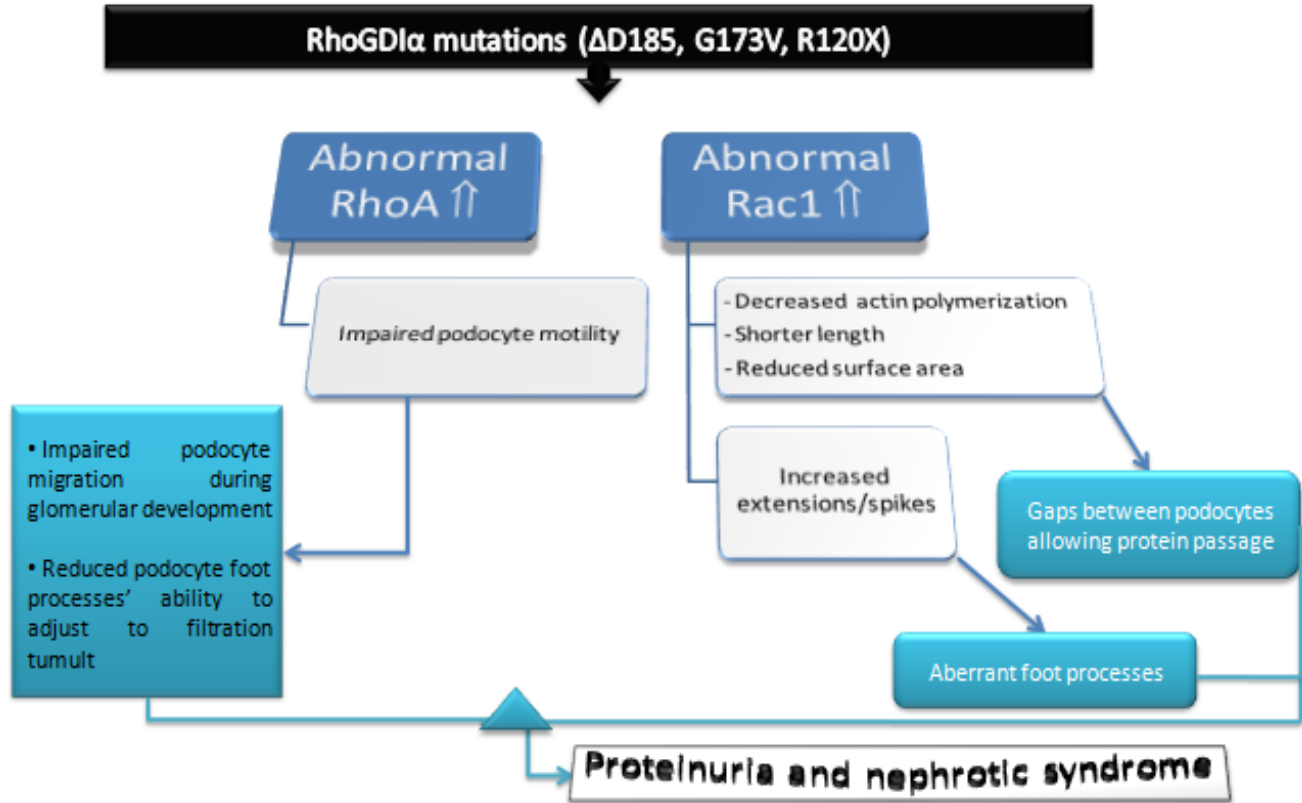


Figure 16: The mutations and Nephrotic Syndrome. The diagram is a recapitulation of our findings and how they translate into Nephrotic Syndrome.

References

1. Gupta, I.R., et al., *ARHGDI1: a novel gene implicated in nephrotic syndrome*. J Med Genet, 2013. **50**(5): p. 330-8.
2. Yoshizaki, H., et al., *Activity of Rho-family GTPases during cell division as visualized with FRET-based probes*. J Cell Biol, 2003. **162**(2): p. 223-32.
3. Elaine Marieb, K.H., *Anatomie et physiologie humaines*, ed. É.d.R. Pédagogique. 2010.
4. Ryan, G.B. and M.J. Karnovsky, *Distribution of endogenous albumin in the rat glomerulus: role of hemodynamic factors in glomerular barrier function*. Kidney Int, 1976. **9**(1): p. 36-45.
5. Deen, W.M., M.J. Lazzara, and B.D. Myers, *Structural determinants of glomerular permeability*. Am J Physiol Renal Physiol, 2001. **281**(4): p. F579-96.
6. Abrahamson, D.R., *Origin of the glomerular basement membrane visualized after in vivo labeling of laminin in newborn rat kidneys*. J Cell Biol, 1985. **100**(6): p. 1988-2000.
7. Schnabel, E., J.M. Anderson, and M.G. Farquhar, *The tight junction protein ZO-1 is concentrated along slit diaphragms of the glomerular epithelium*. J Cell Biol, 1990. **111**(3): p. 1255-63.
8. Neal, C.R., et al., *Glomerular filtration into the subpodocyte space is highly restricted under physiological perfusion conditions*. Am J Physiol Renal Physiol, 2007. **293**(6): p. F1787-98.
9. Hinkes, B.G., et al., *Nephrotic syndrome in the first year of life: two thirds of cases are caused by mutations in 4 genes (NPHS1, NPHS2, WT1, and LAMB2)*. Pediatrics, 2007. **119**(4): p. e907-19.

10. Insall, R.H. and L.M. Machesky, *Actin dynamics at the leading edge: from simple machinery to complex networks*. Dev Cell, 2009. **17**(3): p. 310-22.
11. Mele, C., et al., *MYO1E mutations and childhood familial focal segmental glomerulosclerosis*. N Engl J Med, 2011. **365**(4): p. 295-306.
12. Zhu, L., et al., *Activation of RhoA in podocytes induces focal segmental glomerulosclerosis*. J Am Soc Nephrol, 2011. **22**(9): p. 1621-30.
13. Zhu, J., et al., *p21-activated kinases regulate actin remodeling in glomerular podocytes*. Am J Physiol Renal Physiol, 2010. **298**(4): p. F951-61.
14. Popoff, M.R. and B. Geny, *Multifaceted role of Rho, Rac, Cdc42 and Ras in intercellular junctions, lessons from toxins*. Biochim Biophys Acta, 2009. **1788**(4): p. 797-812.
15. Wong, W., *Idiopathic nephrotic syndrome in New Zealand children, demographic, clinical features, initial management and outcome after twelve-month follow-up: results of a three-year national surveillance study*. J Paediatr Child Health, 2007. **43**(5): p. 337-41.
16. Deschenes, G., V. Guignonis, and A. Doucet, *[Molecular mechanism of edema formation in nephrotic syndrome]*. Arch Pediatr, 2004. **11**(9): p. 1084-94.
17. Wada, T., et al., *Dexamethasone prevents podocyte apoptosis induced by puromycin aminonucleoside: role of p53 and Bcl-2-related family proteins*. J Am Soc Nephrol, 2005. **16**(9): p. 2615-25.
18. Somlo, S. and P. Mundel, *Getting a foothold in nephrotic syndrome*. Nat Genet, 2000. **24**(4): p. 333-5.
19. Jaffe, A.B. and A. Hall, *Rho GTPases: biochemistry and biology*. Annu Rev Cell Dev Biol, 2005. **21**: p. 247-69.

20. Boureux, A., et al., *Evolution of the Rho family of ras-like GTPases in eukaryotes*. Mol Biol Evol, 2007. **24**(1): p. 203-16.
21. Wheeler, A.P. and A.J. Ridley, *Why three Rho proteins? RhoA, RhoB, RhoC, and cell motility*. Exp Cell Res, 2004. **301**(1): p. 43-9.
22. Vincent, S., P. Jeanteur, and P. Fort, *Growth-regulated expression of rhoG, a new member of the ras homolog gene family*. Mol Cell Biol, 1992. **12**(7): p. 3138-48.
23. Ridley, A.J., *Rho GTPases and cell migration*. J Cell Sci, 2001. **114**(Pt 15): p. 2713-22.
24. Gupton, S.L. and F.B. Gertler, *Filopodia: the fingers that do the walking*. Sci STKE, 2007. **2007**(400): p. re5.
25. Neudauer, C.L., et al., *Distinct cellular effects and interactions of the Rho-family GTPase TC10*. Curr Biol, 1998. **8**(21): p. 1151-60.
26. Schmidt, A. and A. Hall, *Guanine nucleotide exchange factors for Rho GTPases: turning on the switch*. Genes Dev, 2002. **16**(13): p. 1587-609.
27. Souchet, M., et al., *Human p63RhoGEF, a novel RhoA-specific guanine nucleotide exchange factor, is localized in cardiac sarcomere*. J Cell Sci, 2002. **115**(Pt 3): p. 629-40.
28. Gao, Y., et al., *Role of RhoA-specific guanine exchange factors in regulation of endomitosis in megakaryocytes*. Dev Cell, 2012. **22**(3): p. 573-84.
29. Zhang, B., L. Yang, and Y. Zheng, *Novel intermediate of Rac GTPase activation by guanine nucleotide exchange factor*. Biochem Biophys Res Commun, 2005. **331**(2): p. 413-21.
30. You, G.Y., et al., *Tiam-1, a GEF for Rac1, plays a critical role in metformin-mediated glucose uptake in C2C12 cells*. Cell Signal, 2013. **25**(12): p. 2558-65.

31. Debreceni, B., et al., *Mechanisms of guanine nucleotide exchange and Rac-mediated signaling revealed by a dominant negative trio mutant*. J Biol Chem, 2004. **279**(5): p. 3777-86.
32. Qin, Y., et al., *Tuba, a Cdc42 GEF, is required for polarized spindle orientation during epithelial cyst formation*. J Cell Biol, 2010. **189**(4): p. 661-9.
33. Datta, A., D.M. Bryant, and K.E. Mostov, *Molecular regulation of lumen morphogenesis*. Curr Biol, 2011. **21**(3): p. R126-36.
34. Lamarche, N. and A. Hall, *GAPs for rho-related GTPases*. Trends Genet, 1994. **10**(12): p. 436-40.
35. Olofsson, B., *Rho guanine dissociation inhibitors: pivotal molecules in cellular signalling*. Cell Signal, 1999. **11**(8): p. 545-54.
36. Thamilselvan, V., M. Menon, and S. Thamilselvan, *Selective Rac1 inhibition protects renal tubular epithelial cells from oxalate-induced NADPH oxidase-mediated oxidative cell injury*. Urol Res, 2012. **40**(4): p. 415-23.
37. Garcia-Mata, R., E. Boulter, and K. Burridge, *The 'invisible hand': regulation of RHO GTPases by RHOGDIs*. Nat Rev Mol Cell Biol, 2011. **12**(8): p. 493-504.
38. DerMardirossian, C., et al., *Phosphorylation of RhoGDI by Src regulates Rho GTPase binding and cytosol-membrane cycling*. Mol Biol Cell, 2006. **17**(11): p. 4760-8.
39. Brunet, N., A. Morin, and B. Olofsson, *RhoGDI-3 regulates RhoG and targets this protein to the Golgi complex through its unique N-terminal domain*. Traffic, 2002. **3**(5): p. 342-57.
40. Grizot, S., et al., *Crystal structure of the Rac1-RhoGDI complex involved in nadph oxidase activation*. Biochemistry, 2001. **40**(34): p. 10007-13.

41. Kestila, M., et al., *Positionally cloned gene for a novel glomerular protein--nephrin--is mutated in congenital nephrotic syndrome*. Mol Cell, 1998. **1**(4): p. 575-82.
42. Togawa, A., et al., *Progressive impairment of kidneys and reproductive organs in mice lacking Rho GDIalpha*. Oncogene, 1999. **18**(39): p. 5373-80.
43. Gee, H.Y., et al., *ARHGDI1 mutations cause nephrotic syndrome via defective RHO GTPase signaling*. J Clin Invest, 2013. **123**(8): p. 3243-53.
44. Shankland, S.J., et al., *Podocytes in culture: past, present, and future*. Kidney Int, 2007. **72**(1): p. 26-36.
45. Wang, L., et al., *Gq-dependent signaling upregulates COX2 in glomerular podocytes*. J Am Soc Nephrol, 2008. **19**(11): p. 2108-18.
46. Zhang, H., et al., *Role of Rho-GTPases in complement-mediated glomerular epithelial cell injury*. Am J Physiol Renal Physiol, 2007. **293**(1): p. F148-56.
47. Aoki, K. and M. Matsuda, *Visualization of small GTPase activity with fluorescence resonance energy transfer-based biosensors*. Nat Protoc, 2009. **4**(11): p. 1623-31.
48. Akilesh, S., et al., *Arhgap24 inactivates Rac1 in mouse podocytes, and a mutant form is associated with familial focal segmental glomerulosclerosis*. J Clin Invest, 2011. **121**(10): p. 4127-37.
49. Tian, D., et al., *Antagonistic regulation of actin dynamics and cell motility by TRPC5 and TRPC6 channels*. Sci Signal, 2010. **3**(145): p. ra77.
50. Asanuma, K., et al., *Synaptopodin orchestrates actin organization and cell motility via regulation of RhoA signalling*. Nat Cell Biol, 2006. **8**(5): p. 485-91.

51. Reiser, J., et al., *Podocyte migration during nephrotic syndrome requires a coordinated interplay between cathepsin L and alpha3 integrin*. J Biol Chem, 2004. **279**(33): p. 34827-32.
52. Gao, Y., et al., *Rational design and characterization of a Rac GTPase-specific small molecule inhibitor*. Proc Natl Acad Sci U S A, 2004. **101**(20): p. 7618-23.
53. Hable, W.E., S. Reddy, and L. Julien, *The Rac1 inhibitor, NSC23766, depolarizes adhesive secretion, endomembrane cycling, and tip growth in the furoid alga, Silvetia compressa*. Planta, 2008. **227**(5): p. 991-1000.